Weathering of microplastics and interaction with other coexisting constituents in terrestrial and aquatic environments

Jiajun Duan [a], Nanthi Bolan [b], Yang Li [a, *], Shiyuan Ding [c], Thilakshani Atugoda [d],

Meththika Vithanage [d], Binoy Sarkar [e], Daniel C.W. Tsang [f], M.B. Kirkham [g]

[a] *Key Laboratory of Water and Sediment Sciences of Ministry of Education, State Key Laboratory of Water Environment Simulation, School of Environment, Beijing Normal University, Beijing 100875, China*

[b] *Global Centre for Environmental Remediation, College of Engineering, Science and Environment, University of Newcastle, Callaghan, NSW 2308, Australia*

[c] *Institute of Surface-Earth System Science, School of Earth System Science, Tianjin University, Tianjin 300072, China*

[d] *Ecosphere Resilience Research Center, Faculty of Applied Sciences, University of Sri Jayewardenepura, Nugegoda 10250, Sri Lanka*

[e] *Lancaster Environment Centre, Lancaster University, Lancaster, LA1 4YQ, UK*

[f] *Department of Civil and Environmental Engineering, The Hong Kong Polytechnic University, Hung Hom, Kowloon, Hong Kong, China*

[g] *Department of Agronomy, Throckmorton Plant Sciences Center, Kansas State University, Manhattan, Kansas 66506, USA*

Corresponding Author

*Phone: +86-10-5880-7612; e-mail: liyang_bnu@bnu.edu.cn (Y.L.).

Highlights

- Sources of microplastics (MPs) are usually linked to anthropogenic activities.

- The weathering rate of MPs is usually lower in water than on land.

- The chemical structure of MPs, oxygen and temperature, control MP weathering.

- Surface modification of weathered MPs affects their environmental behavior.

- MP weathering in soils and sediments needs further research.

31   **Graphical abstract**

32
33
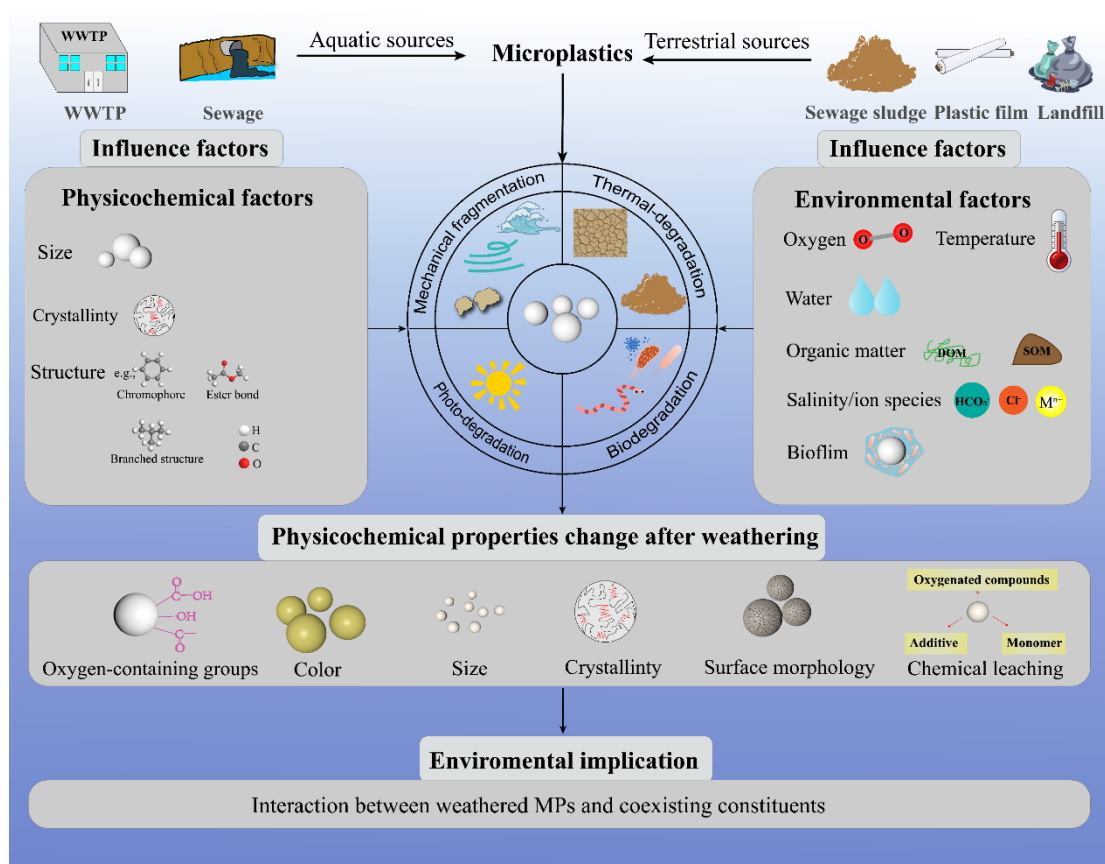
ABSTRACT

Weathering of microplastics (MPs, < 5 mm) in terrestrial and aquatic environments affects MP transport and distribution. This paper first summarizes the sources of MPs, including refuse in landfills, biowastes, plastic films, and wastewater discharge. Once MPs enter water and soil, they undergo different weathering processes. MPs can be converted into small molecules (e.g., oligomers and monomers), and may be completely mineralized under the action of free radicals or microorganisms. The rate and extent of weathering of MPs depend on their physicochemical properties and environmental conditions of the media to which they are exposed. In general, water dissipates heat better, and has a lower temperature, than land; thus, the weathering rate of MPs in the aquatic environment is slower than in the terrestrial environment. These weathering processes increase oxygen-containing functional groups and the specific surface area of MPs, which influence the sorption and aggregation that occur between weathered MPs and their co-existing constituents. More studies are needed to investigate the various weathering processes of diverse MPs under natural field conditions in soils, sediments, and aquatic environments, to understand the impact of weathered MPs in the environment.

Keywords: Microplastics; Aging; Influence factors; Physicochemical property; Aggregation; Sorption

1. Introduction

With the wide application of polymer, more and more particulate plastics have been detected in the environment due to the degradation of bulk plastic polymers and discharge from plastic products (Chen et al., 2019b; Dawson et al., 2018). It has been estimated that the mass of plastics released to land annually (4.73×10^8 - 9.1×10^8 kg) may be 4 to 23 times higher than that released to oceans in the European Union (Horton et al., 2017). Particulate plastics with sizes smaller than 5 mm are defined as microplastics (MPs) (Arthur et al., 2009). By 2100, it is speculated that 2.5×10^7 to 1.3×10^8 tons of MPs float on the ocean surface (Everaert et al., 2018). Sediments are a long-term sink for MPs in deep-sea areas and river-estuary regions (Xu et al., 2020b; Zhang et al., 2020b). Some MPs were found to pose negative impact on organisms, because they may induce oxidative stress and adsorb pollutants, such as heavy metals or organic matters (Ho et al., 2020; Wang et al., 2021b).

The weathering processes of MPs mainly include mechanical fragmentation, photo-degradation, thermal-degradation, and biodegradation (Chen et al., 2019b; Resmeriță et al., 2018; Tu et al., 2020). These abiotic and biotic processes for MP degradation can take hundreds, and even thousands, of years (Iñiguez et al., 2018), depending on the physicochemical properties of MPs and environmental conditions (Chen et al., 2020; Mei et al., 2020; Tian et al., 2019; Turgay et al., 2019; Wang et al., 2020a). However, the combined effects of these factors on various MP weathering processes are complex under natural environmental conditions, which results in unpredictable lifetimes of MPs in the environment. Meanwhile, weathering of MPs influences their interactions with coexisting pollutants (Liu et al., 2019b; Liu et al., 2019d; Wang et al., 2020b), and these interactions need to be summarized to understand

77 the distribution of MPs in the environment and the transport of constituents associated

78 with the MPs.

79   In order to systematically summarize the related research on MP transport and

80 transformation, the Web of Science database was used to retrieve the relevant

81 publications up to February 2021 with the following keywords: microplastics,

82 weathering, source, toxicity, adsorption, aggregation, and deposition. The number of

83 publications that investigated transport and transformation of MPs was 5311. As shown

84 in **Fig. 1**, 46.8% of the research focused on the weathering of MPs, which was more

85 than the research in other areas. Currently, most reviews of MPs have concentrated on

86 the environmental behavior of pristine MPs in water (Mei et al., 2020; Wang et al.,

87 2021a), but has ignored the interaction between weathered MPs and their coexisting

88 constituents in aquatic and terrestrial environments. Additionally, most of these reviews

89 only have summarized a single weathering process (Yuan et al., 2020), without focusing

90 on the influence of multiple weathering processes that affect the fate of MPs.

91   -------------------------------

92   Fig. 1 here

93   -------------------------------

94   This review provides an overview of recent progress in studying weathering of

95 MPs in terrestrial and aquatic environments. To understand fully the weathering

96 processes of MPs and associated factors influencing the weathering in natural

97 environments, the sources of MPs are first described to provide their types,

98 concentrations, and particle sizes in natural waters or soil. Next, the mechanisms of the

99 weathering processes and the main factors that influence them, including the

100 physicochemical properties of MPs and environmental conditions, are summarized.

101 Then how the physicochemical properties are changed during the weathering process

102 is discussed. The section also reviews the interaction between weathered MPs and other

103 coexisting constituents in natural waters or soil. Finally, the knowledge gaps and future

104 recommendations regarding the weathering of MPs are discussed.

105 **2. Sources of particulate plastics enter the environment**

106 The sources of MPs in natural waters or soil are reviewed ahead of the description

107 of their weathering processes to give their types, concentrations, and particle sizes in

108 natural environments. This provides fundamental information for researchers to

109 investigate the weathering processes of MPs under environmentally relevant conditions.

110 **Table 1** shows that most MPs are linked to anthropogenic activities. The common types

111 of MPs consist of polyethylene terephthalate (PET), polypropylene (PP), polyethylene

112 (PE), polyamide (PA), and polystyrene (PS).

113 -------------------------------

114 Table 1 here

115 -------------------------------

116 *2.1. Terrestrial environments*

117 Major sources of terrestrial plastic fragments are from refuse landfills, sewage

118 sludge and plastic films. Solid-waste landfills accumulate 21-42% of global plastic

119 wastes (Nizzetto et al., 2016). Landfill leachate from a municipal solid waste landfill in

120 China had concentrations of MPs with 235.4 ± 17.1 item L^{-1}, and the percentage of tiny

121 MPs smaller than 50 μm was over 50% in landfill leachate (Sun et al., 2021). The

122 sewage sludge retains more than 90% of the MPs that are in the influent wastewater

123 (Zhang et al., 2020a). The recurrent application of the biosolids to agricultural lands

124 (e.g., compost) results in small particles that tend to form secondary MPs and NPs,

125 especially from PE, due to mixing, abrasion, and milling (Kumar et al., 2020). Plastic

126 films have been extensively utilized in agriculture, and the covered agricultural area

127 worldwide is estimated to be around 180,000 km^2 and 13,000 km^2 for plastic mulches

128 and greenhouses, respectively (Xu et al., 2020a). Plastic mulches left on the ground are

129 prone to weathering due to UV light, microbes, and tillage, and they become brittle

130 enough to fall into fragments (Astner et al., 2019). The concentration left in 60% of the

131 agricultural areas in China has exceeded national film residual standard (75 kg ha^{-1}).

132 *2.2. Aquatic environments*

133 Drainage from domestic and industrial wastes is received by wastewater treatment

134 plants (WWTPs), becoming an essential source of MPs in aquatic environments (Da

135 Costa et al., 2018; Li et al., 2020). Household wastewater contains heavy loads of MPs

136 from cosmetics, personal hygiene products, and synthetic fibers from garments.

137 Cosmetic exfoliants release about 4,500 to 94,500 microbeads in a single rinse, of

138 which 90% consist of PE (Napper et al., 2015). Primary and secondary treatment of

139 wastewater at WWTPs can eliminate 70% to 99% of the MPs (Prata, 2018). At a

140 treatment plant in Scotland, even at 98.4% removal efficiency, 65 million particles were

141 discharged into the river Clyde per day with 0.25 items L^{-1} in the final effluent (Murphy

142 et al., 2016). Pedrotti et al. (2021) estimated that 4.3 billion synthetic microfibers were

143 released daily into the marine environment from the Haliotis treatment plant, despite its

144 high removal efficiency (87.5% to 98.5%). In several wastewater treatment facilities

145 across the U.S., the daily number of microplastics discharged to freshwater was

146 estimated to be in the range of 50,000-15,000,000 (Mason et al., 2016). Usually, PS,

147 PE, PET, PA, and PP polymer types dominate in the wastewaters (Murphy et al., 2016;

148 Ziajahromi et al., 2017).

149 *2.3. Particulate-plastics transfer between the terrestrial and aquatic environment*

150   Vertical transfer of MPs leads to their distribution at various depths in the soil. A

151 greater abundance of MPs has been reported in shallow soil than in deeper soil (Liu et

152 al., 2018). Ploughing, soil cracking, and bioturbation caused by earthworms can

153 incorporate MPs in topsoil layers to the 25-cm depth in the soil matrix (Bläsing and

154 Amelung, 2018; Rillig et al., 2017). Soil pores filter out relatively large particles that

155 remain in the surface or near-surface soil, whereas smaller particles (0.1-6.0 µm)

156 presumably pass through the pore channels, and possess greater mobility downwards

157 (Rillig et al., 2017). However, even larger particles (< 1.5 mm) have been found to

158 reach groundwater aquifers due to migration along fractures and crevices in the ground.

159 The occurrence of 12 particles L^{-1} in groundwater has confirmed the vertical transfer in

160 soil (Panno et al., 2019).

161   Erosion can translocate MPs incorporated in the surface or subsurface soil over

162 the ground towards surface water bodies. In particular, arable lands are often vulnerable

163 to movement of MPs by erosion due to high soil permeability, intensive drainage, loss

164 of vegetative cover, and heavy applications of biosolids and compost (Bläsing and

165 Amelung, 2018). In northeast China, the translocation of MPs was claimed to be 96%

166 due to surface-soil water loss (Zhang et al., 2020e). During floods, high tides, and

167 extreme wind conditions, MPs in water can move landwards and become deposited on

168 terrestrial soils. Suspended MPs in rivers and lakes tend to become deposited on

169 floodplains, shorelines, and even remote mountainous areas due to aeolian transport

170 (Scheurer and Bigalke, 2018).

171 **3. Weathering of particulate plastics in terrestrial and aquatic environments**

172   In terrestrial and aquatic environments, MPs will undergo different weathering

173   processes (Auta et al., 2018; He et al., 2018; Iñiguez et al., 2018). The weathering

174   mechanisms based on physical, chemical, and biological reactions have been

175   systematically summarized for the first time in Section 3.2. Additionally, these

176   weathering processes are affected by physicochemical properties of the MPs (e.g., size,

177   structure, and crystallinity) and environmental conditions (e.g., oxygen, water,

178   temperature, and biofilms) (Chen et al., 2020; Mei et al., 2020; Tian et al., 2019; Turgay

179   et al., 2019; Wang et al., 2020a), and they are rarely considered in previous reviews.

180   We compared the effect of physicochemical properties of MPs and environmental

181   conditions on different weathering processes, as discussed in Sections 3.3.1 and 3.3.2,

182   respectively. Recent studies regarding MP weathering processes are summarized in

183   **Table 2**, which shows that most experiments have been conducted under laboratory

184   conditions and are mainly focused on the aquatic environment.

185   -------------------------------

186   Table 2 here

187   -------------------------------

188   **3.1 Weathering processes**

189   *3.1.1. Mechanical fragmentation*

190   Mechanical breakdown originates from abrasion and disintegration forces that are

191   a result of the interaction of MPs with sediments, pebbles, waves, and tide action in

192   aquatic environments. In the terrestrial environment, it can result from human activities

193   (e.g., soil cultivation and crop rotation) (He et al., 2018). As shown in **Table 2**,

194   mechanical fragmentation of MPs has a great possibility of producing more small-sized

195   MPs, even NPs (<10 nm) by simulated sand or wave action. However, the potential

196   disintegration processes, such as freeze-thaw cycles and rainstorm events, are rarely

197   researched. Furthermore, the rate of mechanical fragmentation was promoted by UV

198   irradiation. Song et al. (2017) reported that pristine PP MPs only produced 10.7 ± 0.7

199   particles pellet^{-1} under 2 months of mechanical abrasion, while UV-aged MPs for 12

200   months, after 2-month mechanical abrasion, formed significant amounts of PP

201   fragments ($6,084 \pm 1,061$ particles pellet^{-1}). Therefore, MP accumulation in natural

202   environments will be accelerated under prolonged UV exposure and frequent

203   mechanical wear.

204   *3.1.2. Photo-degradation*

205   Photo-degradation is the major weathering process for most MPs. **Table 2**

206   summarizes recent research about photo-degradation of MPs. The UV fraction of light

207   irradiation plays a key role in MP weathering. UV radiation with a wavelength of 290-

208   400 nm in sunlight has enough energy (299-412 kJ mol^{-1}) to break the C-C bond (284-

209   368 kJ mol^{-1}) and the C-H bond (381-410 kJ mol^{-1}) for most plastics (Kholodovych and

210   Welsh, 2007). Usually, the photo-weathering process mainly occurs on the outer layer

211   of MPs with a µm-range depth, because the high crystallinity of MPs results in light

212   scattering and reflection, which reduces the light penetration distance (ter Halle et al.,

213   2017). To be further oxidized, the weathering layer needs to be removed via mechanical

214   force and a new non-oxidized layer needs to be formed (ter Halle et al., 2017). Moreover,

215   the weathering layer increases surface hydrophily, which enhances microbial adhesion

216   and mineralization rate (Chamas et al., 2020).

217   *3.1.3. Thermal-degradation*

218   Thermal-degradation of MPs leads to bond breakage as a result of overcoming the

219   bond dissociation energy (Pielichowski and Njuguna, 2005). The theoretical maximum

220   temperature of darkish and dry soils has been estimated to be between 90 and 100 °C

221 in natural ground surfaces (Mildrexler et al., 2011; Tang et al., 2019). Therefore, MPs

222 may undergo thermal-degradation processes on land due to the extreme maximal

223 surface ground temperatures. On the contrary, water dissipates heat better and has a

224 lower temperature than dark and dry soils. Thus, thermal-degradation seems to be more

225 important in land than in aquatic environments. It has been demonstrated that thermal

226 weathering (80 ℃, 3 months) of the PE strips was equal to approximately 270 days of

227 UV irradiation at 43-45 ℃ in terrestrial environments (Erni-Cassola et al., 2020). Most

228 studies about MP thermal-degradation kinetics have been conducted at temperatures

229 higher than 300 ℃ in a nitrogen atmosphere (Luo et al., 2020d). The testing

230 environment is greatly inconsistent with the natural environment (e.g., oxygen and

231 temperature). Further studies are needed to explore long-term MP thermal-degradation

232 in natural aquatic or terrestrial systems with environmental temperatures.

233 *3.1.4. Biodegradation*

234   Microbial degradation, and biological ingestion and digestion are main pathways

235 of MP biological weathering. Many plastic-degrading microbial strains have been

236 identified (Chen et al., 2020; Zhang et al., 2020c). As shown in **Table 2**, the degradation

237 efficiency of MPs has ranged from 3.9% to 60%, depending on the species and the

238 diversity of the microbial community. In natural environments, symbiotic and

239 synergistic interactions among microorganisms in bacterial consortia play a major role

240 in MP biodegradation (Yuan et al., 2020). For example, toxic metabolites produced by

241 one microorganism may be used as substrate by another microorganism, thus reducing

242 the influence of the toxic metabolites on MP-degrading bacteria (Yuan et al., 2020).

243 Huerta Lwanga et al. (2018) found that biodegradation of low-density polyethylene

244 (LDPE) MPs by bacterial consortia (phylum Actinobacteria and Firmicutes) separated

245   from the earthworm gut caused a weight loss of 60% and formation of NPs after 21

246   days in soil. Compared with bacterial consortia, a single bacterium has low

247   biodegradation efficiency of MPs (< 15%) after 28-40 days (Auta et al., 2018),

248   indicating bacterial consortia may provide potential solutions for improving

249   biodegradation efficiency of MPs, even though the role of each bacterium in the

250   consortia is unclear. In addition to microbial degradation, PE MPs could rapidly be

251   broken into smaller particles by freshwater amphipod *Gammarus duebeni*, and the

252   fragments accounting for 65.7% of all observed MPs in digestive tracts (Mateos-

253   Cárdenas et al., 2020).

254   **3.2. Weathering mechanisms**

255   *3.2.1. Physical mechanisms*

256   Physical weathering of MPs results in their fragmentation by crack propagation

257   and crack failure under localized shear forces (Enfrin et al., 2020; Julienne et al., 2019a).

258   The defective structures, such as microcracks, are responsible for the initiation of MP

259   fragmentation (Enfrin et al., 2020). Enfrin et al. (2020) used Grady's model regarding

260   the theory of solid failure through crack propagation and fracture to demonstrated that

261   the existing cracks played a determinant role in breaking of MPs into NPs in freshwater.

262   They revealed that longer cracks reduced the minimum stress of crack propagation,

263   thereby resulting in crack failure under further shear forces, which produced a planar

264   exfoliation and NP fragments. Therefore, the generated cracks of MPs during

265   manufacturing or other weathering processes enhance the probability for further

266   fragmentation (Enfrin et al., 2020). Particularly, the destructive effect by crack

267   propagation and failure is more obvious in brittle materials (e.g., PS) in comparison to

268   materials with toughness (e.g., LDPE). It has been demonstrated that 99.8% of PS

269   debris was fragmented into MPs and NPs within 24 h by simulating breaking of waves

270   (Irina et al., 2018). On land, the continuous frictional stresses between tire treads and

271   road surface are mainly responsible for MP generation. When the stress achieves the

272   limiting strength of the rubber material, the tire will be cut or scratched slightly,

273   producing smaller-size particles (Zhang et al., 2021).

274   *3.2.2. Chemical mechanisms*

275   The chemical weathering processes, including photo-degradation and thermal-

276   degradation, can lead to MP chain scission, branching, and generation of oxygenated

277   intermediates via similar radical-based weathering mechanisms (Gardette et al., 2013;

278   Liu et al., 2020c). As shown in **Scheme 1**, the radical-based chemical weathering

279   process is generally divided into three steps, including initiation, propagation, and

280   termination reactions (Yousif and Haddad, 2013). The difference for two chemical

281   weathering processes is the initiator species and weathering products due to the

282   different oxidation efficiencies (Gardette et al., 2013; Liu et al., 2020c).

283   In the initial step, alkyl radicals (R•) are considered as important initiating species

284   (Yousif and Haddad, 2013). For the thermal-degradation process, high temperature

285   overcomes the energy barrier, and causes R• generation via random chain scission at

286   weak sites or chain-end scission of C-C bonds (Singh and Sharma, 2008). For the

287   photodegradation process, the chromophore of MPs absorbs the energy of UV

288   irradiation to become an excited singlet state, which then is transformed into an excited

289   triplet state by intersystem crossing (Yousif and Haddad, 2013). The energy of triplet

290   state of MPs is transferred to the nearest C-C/C-H bonds by intramolecular energy

291   transfer processes, subsequently resulting in chain scission and formation of R•. For

292   example, the excited state of the benzene ring on PS (443 kJ mol^{-1}) has enough energy

293 to cause C-C/C-H bond (< 410 kJ mol^{-1}) rupture (Waldman and De Paoli, 2008). Recent

294 research proved reactive oxide species (ROS) involving the hydroxyl radical (•OH),

295 superoxide radical ($O_2^{•-}$), and singlet oxygen ($^1O_2$) generated by PS MPs play a vital

296 role in their photo-aging (Zhu et al., 2020a). They might promote R• generation via H

297 abstraction from plastic molecule (RH), C-C scission, or phenyl ring opening to

298 accelerate weathering process of MPs (Cho and Choi, 2001).

299 In the propagation step, high-activity radicals, such as •OH, R•, alkoxyl (RO•),

300 and peroxyl (ROO•), can promote self-catalyzed reactions. First, R• react with O_2 and

301 form ROO•, then ROO• abstract the hydrogen atom from another RH or the media (e.g.,

302 H_2O) to form hydroperoxide (ROOH), which will be decomposed into •OH and RO•

303 by absorption of light and heat energy (Tian et al., 2019; Yousif and Haddad, 2013).

304 Subsequently, •OH attack ROOH and RH to form ROO• and R•, respectively (Zweifel,

305 1999). Moreover, the combination of ROO• and RH can form charge transfer (CT)

306 complexes, which through photolysis change into the hydroperoxyl radical (HO$_2$•) and

307 R•. The radical (HO$_2$•) could subsequently form hydrogen peroxide (H_2O_2) (Gugumus,

308 1990). These reactions provide high-activity radicals to keep chain propagation going.

309 The alkoxyl radical is a key intermediate in the reaction and undergoes several reaction

310 pathways, including hydrogen atom abstraction from RH to produce alcohol and β-

311 scission to form ketones or aldehydes (Gewert et al., 2015). Under UV irradiation,

312 ketones undergo successive reactions to produce R• and acyl radicals (R-CO•) by the

313 Norrish I reaction, and to produce the end carbonyl group (R-CO-CH$_3$) by the Norrish

314 II reaction (Gardette et al., 2013).

315 The termination step mainly results in recombination between bimolecular or low

316 molecular radicals, with the main products of ketones, olefins, and aldehydes (Gewert

317   et al., 2015). Additionally, a recent study demonstrated that photo-degradation could

318   result in PS MPs to be completely mineralized into CO_2 under simulated solar

319   irradiation with light intensities of 3 and 10-fold higher than those of natural solar at 0°

320   and 50° north latitude, respectively (Ward et al., 2019). However, the mineralization

321   mechanism of MPs during the photo-aging process needs to be further verified.

322   -------------------------------

323   Scheme 1 here

324   -------------------------------

325   *3.2.3. Biological mechanisms*

326   For microorganisms (mainly bacteria and fungi), the degradation process of MPs

327   is divided into four steps, as shown in **Fig. 2**. First, the microbes adhere and

328   subsequently colonize onto the MP surface. The extracellular polymeric substances

329   (EPS) secreted by microorganisms provide a sticky matrix for the colonization (Ganesh

330   Kumar et al., 2020; Michels et al., 2018). Second, biodeterioration occurs on the MP

331   surface, resulting in physical disintegration of MPs (Lucas et al., 2008). Third, enzymes

332   secreted by microorganisms facilitate the depolymerization process of MPs, which

333   transform MPs into intermediates with smaller molecules (e.g., dipolymers and

334   monomers) and release additives (Yuan et al., 2020). Finally, these small molecular

335   substances and additives, which are used as carbon and energy sources by

336   microorganisms, undergo assimilation, subsequent mineralization, and generation of

337   metabolites (e.g., CO_2, CH_4, and H_2O) (Jacquin et al., 2019).

338   For crustaceans and omnivores, biological ingestion and digestion are considered

339   to be potential biodegradation mechanisms (Dawson et al., 2018; Mateos-Cárdenas et

340   al., 2020). MPs were cut and ground into NPs by mandibles for mastication, and then

341 they were transported into the stomach and gastric mill, which resulted in the

342 fragmentation of plastic particles (Dawson et al., 2018; Mateos-Cárdenas et al., 2020).

343 The digestive enzymes in the stomach might catalyze hydrolytic cleavage of MPs and

344 participate in MP degradation (Mateos-Cárdenas et al., 2020). It is speculated that

345 several enzymes (e.g., amylase, cellulose, esterase, protease, and lipase) from intestinal

346 tracts might be responsible for MP degradation (Song et al., 2020). The contribution of

347 the enzymes to breakdown of MPs and the mechanism of action of the enzymes remain

348 elusive. Furthermore, the interaction between ingested MPs and sharp edges, such as

349 triturated algae, have been shown to accelerate the fragmentation of MPs (Dawson et

350 al., 2018).

351 -------------------------------

352 Fig. 2 here

353 -------------------------------

354 **3.3. Factors affecting weathering processes**

355 *3.3.1. Physicochemical properties of microplastics*

356 *3.3.1.1. Size.* Smaller-sized MPs have a higher specific surface area, and thus provide

357 larger reaction areas for accelerating the fragmentation rate of MPs and leaching rate

358 of chemicals (Luo et al., 2020b; Wang et al., 2020a). In a photo-aging experiment of

359 PVC MPs, the dechlorination efficiency of PVC MPs had a negative correlation with

360 particle size (Wang et al., 2020a). The concentrations of released Cl^- from 2, 10, 25 and

361 150 μm PVC MPs in water were 21.4, 13.2, 10.6 and 7.2 μM after 96 h xenon lamp

362 exposure, respectively (Wang et al., 2020a). However, for semi-crystalline PE

363 particulate plastics with sizes < 500 nm, smaller particles have higher crystallinity and

364 more compactness of polymer chains, thus exhibiting lower thermal-degradation rates

17

365 (Paik and Kar, 2009). For this reason, the weathering rate of MPs not only depends on

366 the specific surface area, but also crystallinity and chain compactness resulting from

367 smaller sizes.

368 *3.3.1.2. Chemical structure.* The chemical structure of MPs is one of the most essential

369 factors determining the weathering rate (Gewert et al., 2015). Chromophore-induced

370 light absorption is the prerequisite for the plastic photo-aging reaction (ter Halle et al.,

371 2017). Thus the dissolved organic carbon (DOC) production and carbon mass loss of

372 PS MPs were faster than other MPs without a chromophore (PP and PE) in seawater

373 (Zhu et al., 2020b). Polyethylene terephthalate MPs are difficult to be biodegraded

374 directly compared to other polyesters, and the main reason for the difficulty is that the

375 aromatic terephthalate units limit the chain mobility, resulting in a low hydrolysis rate

376 of the backbone ester linkages by enzymes (Webb et al., 2012).

377 In addition, the weathering degree is limited by the rate of hydrogen abstraction

378 from plastic molecules or the media (e.g., H_2O) by R• and RO• (as shown in **Scheme**

379 **1**), which is related to the stability of C-H bonds (Hujuri et al., 2008; Song et al., 2017).

380 The dissociation energy of C-H bonds decreases in the order of primary (418 kJ mol^{-}

381 ^{1}) > secondary (402 kJ mol^{-1}) > tertiary (389 kJ mol^{-1}) hydrogen (Wang and Brown,

382 2004). Thus, MPs with tertiary hydrogen (e.g., PS, PP, and PVC) have lower

383 weathering resistance, but MPs without tertiary hydrogen (e.g., PE) are highly stable.

384 For example, the oxidation degree of PP film was approximately 1.75 times faster than

385 that of PE under xenon lamp irradiation (Julienne et al., 2019b). The temperature

386 required for 100% weight loss of PE MPs (495 °C) was found to be higher than that of

387 PP MPs (471 °C) (Hujuri et al., 2008). To reduce the accumulation of polymer with

388 high stability such as PE in environments, it is necessary to investigate their fates to

389   provide an effective remediation strategy.

390   *3.3.1.3. Crystallinity.* Crystallinity of MPs reflects the order degree of the chain

391   structure (Andrady, 2017). The crystalline region has a more tightly and ordered

392   structure than the amorphous region (Mei et al., 2020). Therefore, MPs with high

393   crystallinity have a limited crushing area compared to those with amorphous regions,

394   in which crack propagation, chain scission, and mechanical breakdown occur

395   preferentially (Julienne et al., 2019a). In addition, the direction of crystallite alignment

396   of pristine plastics is in the direction of crack propagation, thereby affecting the shape

397   and number of formed fragments in water under xenon lamp irradiation (Julienne et al.,

398   2019a). Both LDPE and PP MPs had linear crystallite structures perpendicular to the

399   direction of extrusion lines, which caused the direction of crack propagation also to be

400   perpendicular to the extrusion direction, and elongated shapes were formed. Besides,

401   PP had a spherulite structure to allow the propagation of cracks along the radial

402   direction. Eventually, the cracks caused by the linear crystallite and spherulite

403   structures coalesced together, producing fewer elongated and smaller PP fragments

404   than LDPE (Julienne et al., 2019a).

405   *3.3.2. Environmental conditions*

406   *3.3.2.1. Oxygen.* Oxygen plays a dominant role in the photo-, thermal-degradation, and

407   biodegradation of MPs in water and soil. Wang et al. (2020a) confirmed that oxygen

408   might contribute to the photo-dechlorination of PVC MPs. They found that the

409   dechlorination rates of PVC MPs (2 μm) under oxic conditions were 2.8 and 1.8 times

410   higher than those under anaerobic conditions in oxalate and citrate aqueous solutions,

411   respectively (Wang et al., 2020a). Additionally, oxygen can change the metabolic

412   pathway of microorganisms. Under aerobic conditions, microorganisms use oxygen as

413 an electron acceptor, while under anaerobic conditions, they use sulfates, nitrates,

414 carbon dioxide, or metals as electron acceptors (Priyanka and Archana, 2011).

415 Thermodynamically oxygen is a more effective electron acceptor than other substances

416 (Gu, 2003), and, thus, anaerobic conditions may not be conducive to biodegradation.

417 *3.3.2.2. Water.* Water can either promote or inhibit the weathering process of MPs. On

418 the one hand, water could limit oxygen content and prevent UV penetration.

419 Consequently, the photo-aging rate of MPs in pure water is lower than that in air (Cai

420 et al., 2018; Mao et al., 2020; Resmeriță et al., 2018). On the other hand, water plays a

421 prominent role in light scattering and crack propagation. The light scattering of water

422 in a suspension of PS MPs (250 ± 88 nm) increased the light exposure area of the MPs,

423 which promoted the generation of ROO• or R•. They can abstract hydrogen atoms from

424 H_2O to generate ROOH, subsequently decomposing into RO• and •OH and providing

425 more free radicals for the oxidation process (Tian et al., 2019). In addition, water is an

426 essential substance for metabolism, growth, and reproduction of microorganisms; thus,

427 suitable moisture could accelerate the rate of MP biodegradation, especially in the

428 terrestrial environment, by promoting biofilm formation (Grima et al., 2000).

429 *3.3.2.3. Temperature.* Temperature strongly affects mechanical weathering of MPs and

430 the biodegradation rate due to the change of microbial community structure and

431 metabolic activities. High temperature could destroy surface mechanical properties and

432 accelerate the movement of molecules inside MPs and promote the release of additives

433 and monomers (Zhou et al., 2018). Meanwhile, high temperature improved enzymatic

434 activity. Chen et al. (2020) found the mass loss of MPs in sewage sludge was 43.7%

435 after 45 days of composting it using hyperthermophilic composting technology (*h*TC,

436 70 °C), whereas the mass loss was only 4.5% with conventional thermophilic

437　composting (*c*TC, 40 ℃). The predominant genera during the biodegradation of MPs

438　during the *h*TC process were *Thermus* (54.2%), *Bacillus* (24.8%), and *Geobacillus*

439　(19.6%) (Chen et al., 2020). It should be noted that higher temperature (85 ℃) might

440　result in inactivation of most enzymes and decrease the bacterial abundance and

441　diversity, and, thus, it may inhibit the biodegradation of MPs (Chen et al., 2020).

442　*3.3.2.4. Organic matter.* Dissolved organic matter (DOM) in the aquatic environment

443　and soil organic matter (SOM) in the terrestrial environment play important roles in MP

444　photo-degradation and biodegradation (Cai et al., 2018; Liu et al., 2020c). Due to their

445　abundant chromophores (e.g., aromatic rings and carboxyl groups), DOM and SOM

446　serve as photosensitizers and produce hydrated electron, excited triplet states, $O_2^{\bullet-}$, •OH,

447　and $^1O_2$ (Li et al., 2015), which promote the MP photo-aging process. Liu et al. (2019c)

448　suggested that DOM in the Taihu Lake and Yangtze River might be an important factor

449　leading to different photo-aging rates of PP and PS MPs. Furthermore, DOM and SOM

450　are considered as one of the most important carbon sources for microorganisms in water

451　and soil environments (Xue et al., 2012). However, Blöcker et al. (2020) found that PP

452　and LDPE MPs were barely biodegradable in soil. The results might be attributed to

453　the short incubation time (28 days) and low mobility of DOM and SOM in soil (Blöcker

454　et al., 2020). Future work should determine the relationship between DOM/SOM and

455　MP biodegradation at long-term research sites.

456　*3.3.2.5. Salinity and ion species.* Salinity and ion species affect the photo-degradation

457　rate of MPs in the aquatic ecosystem by influencing depth of UV penetration and radical

458　reaction. Increasing salinity results in a high refractive index of water and the formation

459　of attached salt crystals on the MP surface, which, thus, protect MPs from photo-

460　degradation by decreasing the absorption efficiency of light (Cai et al., 2018; Ranjan

461 and Goel, 2019). HCO_3^- and Cl^- are considered as the main ions in freshwater and

462 seawater, respectively (Chen et al., 2019a; Hansard et al., 2011), which can scavenge

463 $\bullet OH$ with reaction constants of $4.3 \times 10^9 \, M^{-1} \, s^{-1}$ and $8.5 \times 10^6 \, M^{-1} \, s^{-1}$, respectively (Liao

464 et al., 2001). Therefore Cl^- and HCO_3^- in natural water might weaken the promotion

465 effect of $\bullet OH$ on photo-aging. However, the common trace metal ions (e.g., iron and

466 manganese) in natural water act as catalysts to oxidize and break MP chains under light

467 irradiation (Leonas, 1993).

468 *3.3.2.6. Biofilm formation.* The surfaces of MPs with various chemical compositions,

469 roughness, and densities can serve as substrates for biofilm formation, especially in

470 aquatic environments (Turgay et al., 2019). Biofilms can either promote the

471 deterioration of the structure of MPs by secreting enzymes and slime matter or inhibit

472 photo-aging and the mechanical breakdown process, because the formed dense layer

473 can shield the surface from light irradiation and shear forces (Yuan et al., 2020). At the

474 same time, biofilms can increase the density of MPs, such as PE MPs, and result in their

475 sinking to the bottom of the water column (Bråte et al., 2018). Settlement further leads

476 to the exposure of MPs to low temperatures and weak light, which may, consequently,

477 inhibit the photo-aging process or thermal-degradation.

478 **4. Impact of weathering on properties of microplastics**

479 *4.1. Surface functional groups*

480   In general, weathering promotes the generation of different oxygen-containing

481 functional groups, mainly C=O, O-H, and C-O on the surface of MPs (Ding et al., 2020;

482 Zhang et al., 2020c). Most studies have used the carbonyl index (CI) and the hydroxyl

483 index (HI), determined by FTIR, to evaluate the weathering degree of MPs (Wu et al.,

484 2020a). The type and generation order of oxygen-containing functional groups depend

485   on the weathering process and environmental conditions. In an aqueous environment,

486   the phenolic hydroxyl group was preferentially formed on the surface of PS MPs,

487   because of excessive hydrogen atoms, while, in a dry environment, the C=O group was

488   more likely to be formed under UV irradiation (Mao et al., 2020). Moreover, under

489   UVB irradiation for 12 months, the surface of PP MPs evolved into O-H and C=O

490   groups, but only the O-H group was observed after thermal weathering at 50 °C for 12

491   months or at 100 °C for 6 months (Tang et al., 2019).

492   *4.2. Color change*

493   Most MPs can undergo visible color changes, which is considered as an intuitive

494   indicator of weathering behavior (Luo et al., 2020d). A colorimeter is applied to

495   measure the color intensity of pristine and weathered MPs based on the CIE 1976 L^*a^*

496   b^* color system (Robertson, 1977). An increase in the value of L^* indicates that the

497   color of MPs is lightening (Robertson, 1977). The color coordinates a^* and b^* represent

498   the red/green coordinate and the yellow/blue coordinate, respectively (Robertson,

499   1977). The total color change (ΔE^*) of MPs is calculated and considered as an index of

500   color change according to Equation (1) (Robertson, 1977):

501 $$\Delta E^* = \sqrt{(\Delta L^*)^2 + (\Delta a^*)^2 + (\Delta b^*)^2} \tag{1}$$

502   where ΔL^*, Δa^*, and Δb^* are the differences between pristine and weathered values of

503   L^*, a^*, and b^*, respectively.

504   A laboratory study demonstrated that the ΔE^* value of pristine PE MPs increased

505   drastically from 0 to 8.4 after a 6-week exposure to a xenon lamp (Luo et al., 2020d).

506   This phenomenon indicated that the chromaticity of MPs was primarily correlated with

507   the oxidation reaction (Luo et al., 2020d). During the chemical weathering process,

508   yellow discoloration is a common aging result for most of the white, off white, or

509   translucent MPs, which is attributed to the formation of chromophores during the aging

510   process (Battulga et al., 2020). For example, phenolic antioxidants in MPs are oxidized

511   into by-products with quinoidal structures that result in a yellow discoloration of MPs

512   (Battulga et al., 2020).

513   *4.3. Size and surface morphology*

514   The decrease in particle size and increase in surface roughness are frequently

515   observed for weathered MPs (Liu et al., 2019c; Song et al., 2017). The mechanical

516   forces from wave, wind, and sand abrasion lead to the loss of mechanical stability, in

517   which the tensile strength of MPs is an important factor (Liu et al., 2019c; Song et al.,

518   2017). As shown in **Fig. 3a-c**, the photo-aging process causes the formation of a brittle

519   surface and cracks on the MP surface, which can accelerate the fragmentation rate after

520   the action of physical forces. After exposure to UV (12 months) and subsequent

521   mechanical abrasion (2 months), the fragment number of LDPE, PP, and expanded PS

522   was 699, 569, and 2 times more than those with only mechanical abrasion for 2 months,

523   respectively. Moreover, SEM images of aged PP MPs showed obvious pits,

524   microcracks, grooves, or broken edges on their surfaces, as shown in **Fig. 3d** (Song et

525   al., 2017). Correspondingly, the mean particle size of MPs decreased along with the

526   increase in the number of fragments (Zhu et al., 2020a).

527   -------------------------------

528   Fig. 3 here

529   -------------------------------

530   *4.4. Crystallinity*

531   An increase in crystallinity can be considered as an index of the weathering of

532   MPs (Wu et al., 2020a). Weathering preferentially degrades the amorphous portion of

533   plastics, thus increasing the percentage of the crystallization region (McGivney et al.,

534 2020). The shorter chains from chain scission can crystallize more readily than longer

535 chains due to their higher mobility, and this accelerates the re-crystallization process in

536 later stages of the weathering process (Andrady, 2017; Julienne et al., 2019a). The

537 degree of crystallinity of MPs is measured by an X-ray diffractometer (XRD) and

538 differential scanning calorimetry (DSC) (McGivney et al., 2020; Wu et al., 2020a). The

539 XRD patterns shown in **Fig. 4** indicated that the weathering process improved the

540 crystallinity of PS MPs, which increased in the order of pristine PS (62.5%) < seawater-

541 aged PS (63.9%) < UV-aged PS in seawater (65.0%) < UV-aged PS (66.8%) (Wu et al.,

542 2020a). Moreover, the DSC exotherms revealed that the presence of biofilms increased

543 the crystallinity of PE MPs by 3.2% (McGivney et al., 2020).

544 -------------------------------

545 Fig. 4 here

546 -------------------------------

547 *4.5. Leaching of chemicals*

548 Weathering of MPs can leach chemicals, such as additives, monomers, and

549 oxygenated intermediates, as shown in **Table 3** (Luo et al., 2020b; Zhang et al., 2019;

550 Zhu et al., 2020b). The released additives mainly include endocrine disrupting

551 chemicals (EDCs) (e.g., phthalate and BPS) and metal ions (e.g., Cr^{6+} and Pb^{2+}) in the

552 aqueous environment. Dissolved organic carbon and CO_2 were major by-products of

553 MPs through chain scission and oxidation reactions in an aquatic environment under

554 UV irradiation (Ward et al., 2019; Zhu et al., 2020b). In addition, light irradiation

555 promotes chemical leaching, because the formation of cracks and fragments in the

556 weathered MPs provides a larger contact area for chemicals with oxygen or for the

557 aqueous solution (Luo et al., 2020b). For MPs sampled from the North Pacific Gyre,

558 the leaching rate of DOC in light (0.235 ± 0.003 mg g^{-1} d^{-1}) was 10 times faster than

559 that in the dark (Zhu et al., 2020b). By contrast, other studies reported that UV

560 irradiation decreased the concentrations of some released chemicals (such as organotin

561 and DOC), because of their photodegradation, volatilization, and reabsorption onto the

562 MP surface (Chen et al., 2019a; Romera-Castillo et al., 2018).

563 ------------------------------

564   Table 3 here

565 ------------------------------

566 **5. Interactions between weathered microplastics and coexisting constituents**

567   The increased surface area and hydrophilicity of weathered MPs are of great

568 importance for the interaction between weathered MPs and other coexisting

569 constituents, which includes adsorption of inorganic/organic contaminants and homo-

570 /hetero-aggregation with other coexisting solid constituents (Liu et al., 2019b; Liu et

571 al., 2020b; Wang et al., 2020b). These weathering-induced environmental behaviors

572 further affect transport and bioavailability to organisms of MPs (Liu et al., 2019b).

573 *5.1. Sorption of inorganic contaminants*

574   Weathered microplastics can promote the absorption of potentially toxic elements

575 including heavy metals and metalloids via ion complexation, hydrogen bonding, and

576 electrostatic interaction forces as shown in **Fig. 5** (Dong et al., 2020; Wang et al.,

577 2020b). Weathered MPs have a positive correlation between their adsorption capacities

578 for the inorganic contaminants and CI values in aqueous solution, indicating that the

579 degree of weathering of MPs influences the adsorption ability of heavy metal ions and

580 metalloid ions (Mao et al., 2020; Wang et al., 2020b; Yang et al., 2019). A 1.6-fold

581 increase of equilibrium Zn^{2+} adsorption capacity was observed by 300 h UV-aged PET

582 MPs (86.8 μg g^{-1}) over the pristine MPs (54.7 μg g^{-1}) in aqueous solution (Wang et al.,

583 2020b). The higher adsorption capacities of weathered MPs are principally due to the

584 following three reasons: (1) increased chapped, wrinkled, and rough surfaces of

585 weathered MPs provide more active sites than pristine MPs for contaminants (Fu et al.,

586 2019; Wang et al., 2020b), (2) oxygen-containing functional groups strengthen the

587 interaction forces between MPs and metal cations by ion complexation and hydrogen

588 bonding (Brennecke et al., 2016; Mao et al., 2020), and (3) increased electronegativity

589 on aged MP surfaces enables greater electrostatic attraction between metal cations and

590 MPs (Yang et al., 2019).

591   In addition, biofilms on weathered MPs have been shown to act as vectors of metal

592 cations. The EPS in biofilms include O-H and C=O groups, promoting Cu^{2+} adsorption

593 onto the surface of PE MPs via complexation (Wang et al., 2020d), which highlights

594 the probable effect of biofilms on migration and transformation of inorganic

595 contaminants in the environment. Biofilm coverage can change the mechanism of Cu^{2+}

596 diffusion from intra-particle diffusion of pristine MPs into film diffusion of aged MPs,

597 which facilitates Cu^{2+} adsorption (Wang et al., 2020d).

598 *5.2. Sorption of organic contaminants*

599   As shown in **Fig. 5**, hydrogen bonding and electrostatic interaction play dominant

600 roles for sorption of hydrophilic organic contaminants (e.g., tetracycline and

601 ciprofloxacin) on weathered surfaces of MPs due to increased oxygen-containing

602 functional groups, high hydrophilicity, and electronegativity (Liu et al., 2019a; Wu et

603 al., 2020b). Compared to pristine MPs, the maximum adsorption capacity of

604 tetracycline and ciprofloxacin on UV-aged PLA MPs increased by 2.2 (from 2.5 to 5.5

605 mg g^{-1}) and 1.2 (from 3.2 to 3.8 mg g^{-1}) fold, respectively (Fan et al., 2021). On the

606　contrary, a decrease of hydrophobic interaction forces is the primary reason for lower

607　adsorption capacity for hydrophobic organic contaminants (HOC) on weathered MPs.

608　For example, the equilibrium sorption capacity of 2,2',4,4'-tetrabromodiphenyl ether

609　(BDE-47) on UV-aged PS MPs (3.75 ng g^{-1}) decreased to half of that for the pristine

610　PS (6.16 ng g^{-1}) (Wu et al., 2020a). In addition, π-π interaction was shown to be the key

611　interaction mechanism between pristine PS MPs and aromatic compounds. Although

612　the π-π interaction might be weakened due to the opening of phenyl rings of PS MPs

613　during the UV aging process (Liu et al., 2020b; Liu et al., 2020c), the interaction seems

614　to play a minor role compared with the above interaction forces on weathered MPs.

615　-------------------------------

616　Fig. 5 here

617　-------------------------------

618　*5.3. Homo-aggregation or hetero-aggregation with other solid particles*

619　*5.3.1. Homo-aggregation of weathered MPs*

620　　　　Weathered MPs can influence their aggregation behavior mainly by changing

621　hydrophilic interaction, electrostatic interaction, van der Waals interactions, and

622　biofilm formation (**Fig. 6**). Ultraviolet irradiation inhibited the homo-aggregation of PS

623　NPs (50-100 nm) in NaCl solutions, which was primarily because the formed oxygen-

624　containing functional groups on the PS NP surface improved the electrostatic repulsion

625　between two approaching particles (Liu et al., 2019d). Similar phenomena were

626　observed in the soil environment (Liu et al., 2019b). Under UV irradiation, the surface

627　oxidation of PS NPs increased their negative charges and hydrophilicity in saturated

628　loamy sand, thus decreasing the aggregation of MPs (Liu et al., 2019b).

629　　　　By contrast, UV light promoted the aggregation of aged PS NPs in CaCl$_2$ solutions,

630 which resulted from the bridging effect between the formed oxygen-containing

631 functional groups and Ca^{2+} (Liu et al., 2019d). In water environments, most of the MP

632 surfaces were covered by biofilms, which secreted sticky EPS served as tackiness

633 agents, which subsequently accelerating homo-aggregation of MPs (Michels et al.,

634 2018). Additionally, NPs formed by MP fragmentation via mechanical weathering (e.g.,

635 shear forces) were prone to homo-aggregation, which was attributed to the increased

636 surface energy. Nanoplastics with high surface energy tended to aggregate to minimize

637 their Gibbs free energy and reached a stable state (Enfrin et al., 2020). However, the

638 aggregates were readily dispersed by repeated shear forces, due to their low cohesion

639 forces (low van der Waals force) (Enfrin et al., 2020).

640 *5.3.2. Hetero-aggregation of weathered MPs with other particles*

641 Weathering of MPs has a greater impact on hetero-aggregation of MPs with other

642 solid particles than homo-aggregation due to the abundance of coexisting solid

643 constituents in the natural environment (Alimi et al., 2018). Michels et al. (2018)

644 investigated the effect of biofilms on the hetero-aggregation between PE MPs and

645 biogenic particles (phytoplankton) in the aquatic environment. With the naked eye, they

646 were able to observe hetero-aggregate formation by pristine PS MPs in seawater with

647 phytoplankton after one day, while biofilm-covered PS MPs hetero-aggregates with

648 biogenic particles were obvious just after a few hours. However, the interaction of

649 weathered MPs with other solid particles (e.g., suspended sediments and microalgae)

650 in water has yet to be elucidated.

651 -------------------------------

652 Fig. 6 here

653 -------------------------------

6. Knowledge gaps and future recommendations

6.1. Evaluate the weathering process under actual environmental conditions

Most published studies have concentrated on investigating the weathering of MPs under laboratory-simulated environments (Chen et al., 2019a; Enfrin et al., 2020; Luo et al., 2020c), and only a few studies have focused on the weathering of MPs under natural environmental conditions (Chen et al., 2020; Tu et al., 2020). Even though weathering phenomena and mechanisms have been concluded from these studies, it is controversial whether the laboratory-simulated conditions represent environmentally relevant systems. For example, photo-weathering experiments with MPs commonly use a xenon lamp to simulate sunlight. However, the latitude, longitude, solar elevation angle, and meteorological conditions determine the intensity and spectral distribution of sunlight (Casado et al., 2019), which cause the difference between MP weathering with a xenon lamp and natural sunlight. Some potential influencing factors (e.g., ions, natural organic matter, and plant secretions) might exert an influence on the MP weathering. Furthermore, most MPs undergo various weathering processes at the same time in natural environments, which results in complexity and uncertainty of the weathering behavior and mechanisms. Considering the complexity of natural systems and the weathering processes, future studies should explore multiple weathering behaviors and mechanisms of MPs under actual aquatic or terrestrial environmental conditions.

6.2. Consider the effect of microplastic diversity on weathering

Most weathering studies of MPs have used traditional and spherical plastic particles, such as PP, PS, PE, PVC, and PET. Recently, MPs with irregular shape and new plastics, including biodegradable MPs (e.g., polyhydroxy butyrate) and functional

678   MPs (e.g., carboxyl-modified PS), are being released into natural environments

679   (Gonzalez-Pleiter et al., 2019; Wang et al., 2020c), and they have been rarely

680   considered in weathering studies. Meanwhile, different types of MPs co-exist in the

681   field. However, only a single type of MPs is used in weathering experiments, which

682   ignores the mutual influence or competition among MPs. For instance, the excited state

683   of benzene ring (4.59 eV) on PS could transfer energy to the excited state of the

684   carbonyl (4.09 eV) on PP by an intramolecular energy transfer process. Then the energy

685   can break the C-H bond of PP, generating more high-activity tertiary carbon radicals

686   under UV irradiation (Waldman and De Paoli, 2008). More research should be carried

687   out using new synthetic, irregularly shaped, and mixed MPs as model particles, to

688   provide a more reasonable understanding of MP weathering.

689   *6.3. Improve the understanding of the weathering process in soils or sediments*

690   Factors influencing the weathering processes of MPs have been mainly studied in

691   aquatic environments with little attention paid to terrestrial environments. In addition

692   to biological phenomena, mechanical degradation, photo-degradation, and thermal-

693   degradation may also influence the distribution and fate of MPs in soils. Research

694   investigating the influence of soil conditions (e.g., moisture content, mineral materials,

695   microbial species, and soil physico-chemical parameters) on the MP weathering

696   processes is urgently needed. Previous studies have suggested that sediments in the

697   ocean and river estuaries accumulate MPs and become long-term sinks for MPs (Xu et

698   al., 2020b; Zhang et al., 2020b). The anaerobic environment and special microbial

699   habitat of sediments may result in MPs undergoing anaerobic biodegradation and

700   mechanical fragmentation. It is of great importance to focus on the weathering

701   processes of MPs in soils or sediments, where the low oxygen content and weak light

702   intensity may limit the extent of photo-weathering reactions.

703   *6.4. Strengthen research on the interaction between weathered MPs and coexisting*

704   *constituents*

705   In water environments, the stability and mobility of MPs change during the aging

706   process, because of altered zeta potentials, surface areas, roughness, and

707   hydrophobicity (Wang et al., 2020b; Wu et al., 2020a). These altered physicochemical

708   properties may also influence the interaction of MPs with other solid particles. Hetero-

709   aggregation of weathered MPs in water remains elusive. How and whether the aging

710   process interferes with homo-aggregation and hetero-aggregation of weathered MPs

711   with other particles in terrestrial environments are unknown, due to the lack of

712   separation, identification, and quantification methods for particle size of MP aggregates.

713   Research regarding the interaction of weathered MPs with other pollutants has mainly

714   concentrated on the sorption of a single heavy metal or organic matter (Dong et al.,

715   2020; Wang et al., 2020b). Competitive adsorption of weathered MPs for mixed

716   pollutants needs to be studied, because many heavy metals and organic pollutants co-

717   exist in natural environments. Weathered MPs can release additives, monomers, or

718   oxygenated intermediates, which may be reabsorbed onto the surfaces of MPs (Liu et

719   al., 2020b). Further work is needed to better understand the effect of the reabsorption

720   process on heavy metals and organic pollutants.

721   *6.5. Concern MP weathering process in waste water*

722   Most previous research has concentrated on the weathering of MPs in natural

723   water, and, sporadically, research has considered the soil, but ignored the weathering

724   process in waste water (e.g., landfill leachates), which is also a major source of MPs.

725   Large amounts of plastic waste disposed in landfills or dumpsites are subjected to

726 multiple weathering processes, which depend upon leachate pH (4.5-9), salinity,

727 concentration of heavy metals and organic pollutants, and bacterial communities (He et

728 al., 2019; Sun et al., 2021). For example, the transition metals in landfills or leachates

729 (e.g., Fe and Cu) might promote the decomposition of organic molecules (e.g., ROOH),

730 and thus accelerate polymer weathering (Hou et al., 2021). Further research is needed

731 to investigate the weathering processes in waste water under the influence of complex

732 field conditions that are different from those in the natural, ambient environment (e.g.,

733 surface water).

734 **7. Conclusions**

735 The weathering of MPs is an important process determining their transport,

736 transformation, and interactions with contaminants and microorganisms in water and

737 soil. Sources of MPs are usually linked to anthropogenic activities including refuse in

738 landfills, biowaste application, plastic film utilization, and wastewater discharge.

739 Microplastics undergo various weathering processes, including mechanical

740 fragmentation, photo-degradation, thermal- degradation, and biodegradation. The

741 physicochemical properties of MPs and environmental conditions affect the degree of

742 their weathering. Generally, MPs, which have a small size and large specific surface

743 area, provide many reaction sites; MPs with a low degree of crystallinity facilitate the

744 diffusion of oxygen, water molecules, and radicals, which accelerate the weathering

745 rate. However, some factors have opposing effects on the weathering of MPs. For

746 example, biofilm formation on MP surfaces promotes plastic biodegradation, but

747 inhibits photo-degradation. The surface-property modification of MPs resulting from

748 weathering strongly affects the sorption or aggregation of weathered MPs and other

749 coexisting constituents by influencing interactive forces, such as hydrogen bond

750 interaction, hydrophilic interaction, electrostatic interaction, and van der Waals

751 interactions. To predict fully the fate and environmental interactions of MPs, more

752 knowledge is needed concerning the *in-situ* weathering behavior of different types of

753 MPs that co-exist in natural aquatic and terrestrial environments.

754 **Declaration of Competing Interest**

755 The authors declare that they have no known competing financial interests or

756 personal relationships that could appear to influence the work reported in this paper.

757 **Acknowledgements**

763   **References**

764   Alimi, O.S., Farner Budarz, J., Hernandez, L.M., Tufenkji, N., 2018. Microplastics and

765   nanoplastics in aquatic environments: aggregation, deposition, and enhanced

766   contaminant transport. Environ. Sci. Technol. 52 (4), 1704-1724.

767   doi:10.1021/acs.est.7b05559.

768   Andrady, A.L., 2017. The plastic in microplastics: a review. Mar. Pollut. Bull. 119 (1),

769   12-22. doi:10.1016/j.marpolbul.2017.01.082.

770   Arthur, C., Baker, J., Bamford, H., 2009. In: Proceedings of the International Research

771   Workshop on the Occurrence, Effects, and Fate of Microplastic Marine Debris.

772   September 9-11, 2008.

773   Astner, A.F., Hayes, D.G., O'Neill, H., Evans, B.R., Pingali, S.V., Urban, V.S., Young,

774   T.M., 2019. Mechanical formation of micro- and nano-plastic materials for

775   environmental studies in agricultural ecosystems. Sci. Total. Environ. 685, 1097-

776   1106. doi:10.1016/j.scitotenv.2019.06.241.

777   Ateia, M., Kanan, A., Karanfil, T., 2020. Microplastics release precursors of chlorinated

778   and brominated disinfection byproducts in water. Chemosphere 251, 126452.

779   doi:10.1016/j.chemosphere.2020.126452.

780   Auta, H.S., Emenike, C.U., Jayanthi, B., Fauziah, S.H., 2018. Growth kinetics and

781   biodeterioration of polypropylene microplastics by *Bacillus* sp. and *Rhodococcus*

782   sp. isolated from mangrove sediment. Mar. Pollut. Bull. 127, 15-21.

783   doi:10.1016/j.marpolbul.2017.11.036.

784   Battulga, B., Kawahigashi, M., Oyuntsetseg, B., 2020. Behavior and distribution of

785   polystyrene foams on the shore of Tuul River in Mongolia. Environ. Pollut. 260,

786   113979. doi:10.1016/j.envpol.2020.113979.

787   Bläsing, M., Amelung, W., 2018. Plastics in soil: analytical methods and possible

788   sources. Sci. Total. Environ. 612, 422-435. doi:10.1016/j.scitotenv.2017.08.086.

789   Blöcker, L., Watson, C., Wichern, F., 2020. Living in the plastic age-Different short-

790   term microbial response to microplastics addition to arable soils with contrasting

791   soil organic matter content and farm management legacy. Environ. Pollut., 115468.

792   doi:10.1016/j.envpol.2020.115468.

793   Bråte, I.L.N., Blázquez, M., Brooks, S.J., Thomas, K.V., 2018. Weathering impacts the

794   uptake of polyethylene microparticles from toothpaste in Mediterranean mussels

795   (*M. galloprovincialis*). Sci. Total. Environ. 626, 1310-1318.

796   doi:10.1016/j.scitotenv.2018.01.141.

797   Brennecke, D., Duarte, B., Paiva, F., Caçador, I., Canning-Clode, J., 2016.

798   Microplastics as vector for heavy metal contamination from the marine

799   environment. Estuar. Coast. Shelf. S. 178, 189-195.

800   doi:10.1016/j.ecss.2015.12.003.

801   Cai, L., Wang, J., Peng, J., Wu, Z., Tan, X., 2018. Observation of the degradation of

802   three types of plastic pellets exposed to UV irradiation in three different

803   environments. Sci. Total. Environ. 628, 740-747.

804   doi:10.1016/j.scitotenv.2018.02.079.

805   Casado, C., García-Gil, Á., van Grieken, R., Marugán, J., 2019. Critical role of the light

806   spectrum on the simulation of solar photocatalytic reactors. Appl Catal B-Environ.

807   252, 1-9. doi:10.1016/j.apcatb.2019.04.004.

808   Chamas, A., Moon, H., Zheng, J., Qiu, Y., Tabassum, T., Jang, J.H., Abu-Omar, M.,

809   Scott, S.L., Suh, S., 2020. Degradation rates of plastics in the environment. ACS

810   Sustain. Chem. Eng. 8 (9), 3494-3511. doi:10.1021/acssuschemeng.9b06635.

811   Chen, C., Chen, L., Yao, Y., Artigas, F., Huang, Q., Zhang, W., 2019a. Organotin

812   release from polyvinyl chloride microplastics and concurrent photodegradation in

813   water: impacts from salinity, dissolved organic matter, and light exposure. Environ.

814   Sci. Technol. 53 (18), 10741-10752. doi:10.1021/acs.est.9b03428.

815   Chen, Q., Allgeier, A., Yin, D., Hollert, H., 2019b. Leaching of endocrine disrupting

816   chemicals from marine microplastics and mesoplastics under common life stress

817   conditions. Environ. Int. 130, 104938. doi:10.1016/j.envint.2019.104938.

818   Chen, Z., Zhao, W., Xing, R., Xie, S., Yang, X., Cui, P., Lü, J., Liao, H., Yu, Z., Wang,

819   S., Zhou, S., 2020. Enhanced in situ biodegradation of microplastics in sewage

820   sludge using hyperthermophilic composting technology. J. Hazard. Mater. 384,

821   121271. doi:10.1016/j.jhazmat.2019.121271.

822   Cho, S., Choi, W., 2001. Solid-phase photocatalytic degradation of PVC–TiO$_2$ polymer

823   composites. J. Photoch. Photobio. A. 143 (2), 221-228. doi:10.1016/S1010-

824   6030(01)00499-3.

825   Corradini, F., Meza, P., Eguiluz, R., Casado, F., Huerta-Lwanga, E., Geissen, V., 2019.

826   Evidence of microplastic accumulation in agricultural soils from sewage sludge

827   disposal. Sci. Total. Environ. 671, 411-420. doi:10.1016/j.scitotenv.2019.03.368.

828   Da Costa, J.P., Nunes, A.R., Santos, P.S.M., Girão, A.V., Duarte, A.C., Rocha-Santos,

829   T., 2018. Degradation of polyethylene microplastics in seawater: insights into the

830   environmental degradation of polymers. J. Environ. Sci. Health, Part A 53 (9),

831   866-875. doi:10.1080/10934529.2018.1455381.

832   Dawson, A.L., Kawaguchi, S., King, C.K., Townsend, K.A., King, R., Huston, W.M.,

833   Bengtson Nash, S.M., 2018. Turning microplastics into nanoplastics through

834   digestive fragmentation by Antarctic krill. Nat. Commun. 9 (1), 1001.

835   doi:10.1038/s41467-018-03465-9.

836   Ding, L., Mao, R., Ma, S., Guo, X., Zhu, L., 2020. High temperature depended on the

837   ageing mechanism of microplastics under different environmental conditions and

838   its effect on the distribution of organic pollutants. Water Res. 174, 115634.

839   doi:10.1016/j.watres.2020.115634.

840   Dong, Y., Gao, M., Song, Z., Qiu, W., 2020. As(III) adsorption onto different-sized

841   polystyrene microplastic particles and its mechanism. Chemosphere 239, 124792.

842   doi:10.1016/j.chemosphere.2019.124792.

843   Enfrin, M., Lee, J., Gibert, Y., Basheer, F., Kong, L., Dumée, L.F., 2020. Release of

844   hazardous nanoplastic contaminants due to microplastics fragmentation under

845   shear   stress   forces.   J.   Hazard.   Mater.   384,   121393.

846   doi:10.1016/j.jhazmat.2019.121393.

847   Erni-Cassola, G., Wright, R.J., Gibson, M.I., Christie-Oleza, J.A., 2020. Early

848   colonization of weathered polyethylene by distinct bacteria in marine coastal

849   seawater. Microb. Ecol. 79 (3), 517-526. doi:10.1007/s00248-019-01424-5.

850   Everaert, G., Van Cauwenberghe, L., De Rijcke, M., Koelmans, A.A., Mees, J.,

851   Vandegehuchte, M., Janssen, C.R., 2018. Risk assessment of microplastics in the

852   ocean: Modelling approach and first conclusions. Environ. Pollut. 242, 1930-1938.

853   doi:10.1016/j.envpol.2018.07.069.

854   Fan, X., Zou, Y., Geng, N., Liu, J., Hou, J., Li, D., Yang, C., Li, Y., 2021. Investigation

855   on the adsorption and desorption behaviors of antibiotics by degradable MPs with

856   or   without   UV   ageing   process.   J.   Hazard.   Mater.   401,   123363.

857   doi:10.1016/j.jhazmat.2020.123363.

858   Fu, D., Zhang, Q., Fan, Z., Qi, H., Wang, Z., Peng, L., 2019. Aged microplastics

859   polyvinyl chloride interact with copper and cause oxidative stress towards

860   microalgae *Chlorella vulgaris*. Aquat. Toxicol. 216, 105319.

861   doi:10.1016/j.aquatox.2019.105319.

862   Ganesh Kumar, A., Anjana, K., Hinduja, M., Sujitha, K., Dharani, G., 2020. Review on

863   plastic wastes in marine environment-biodegradation and biotechnological

864   solutions. Mar. Pollut. Bull. 150, 110733. doi:10.1016/j.marpolbul.2019.110733.

865   Gardette, M., Perthue, A., Gardette, J.-L., Janecska, T., Földes, E., Pukánszky, B.,

866   Therias, S., 2013. Photo- and thermal-oxidation of polyethylene: comparison of

867   mechanisms and influence of unsaturation content. Polym. Degrad. Stabil. 98 (11),

868   2383-2390. doi:10.1016/j.polymdegradstab.2013.07.017.

869   Gewert, B., Plassmann, M.M., MacLeod, M., 2015. Pathways for degradation of plastic

870   polymers floating in the marine environment. Environ. Sci. Process. Impacts 17

871   (9), 1513-1521. doi:10.1039/c5em00207a.

872   Gonzalez-Pleiter, M., Tamayo-Belda, M., Pulido-Reyes, G., Amariei, G., Leganes, F.,

873   Rosal, R., Fernandez-Pinas, F., 2019. Secondary nanoplastics released from a

874   biodegradable microplastic severely impact freshwater environments. Environ.

875   Sci. Nano 6 (5), 1382-1392. doi:10.1039/c8en01427b.

876   Grima, S., Bellon-Maurel, V., Feuilloley, P., Silvestre, F., 2000. Aerobic

877   biodegradation of polymers in solid-state conditions: A review of environmental

878   and physicochemical parameter settings in laboratory simulations. J. Polym.

879   Environ. 8 (4), 183-195. doi:10.1023/A:1015297727244.

880   Gu, J.-D., 2003. Microbiological deterioration and degradation of synthetic polymeric

881   materials: Recent research advances. Int. Biodeter. Biodegr. 52 (2), 69-91.

882   doi:10.1016/S0964-8305(02)00177-4.

883   Gugumus, F., 1990. Mechanisms of photooxidation of polyolefins. Angew. Makromol.

884   Chem. 176 (1), 27-42. doi:10.1002/apmc.1990.051760102.

885   Hansard, S.P., Easter, H.D., Voelker, B.M., 2011. Rapid reaction of nanomolar Mn(II)

886   with superoxide radical in seawater and simulated freshwater. Environ. Sci.

887   Technol. 45 (7), 2811-2817. doi:10.1021/es104014s.

888   He, D., Luo, Y., Lu, S., Liu, M., Song, Y., Lei, L., 2018. Microplastics in soils:

889   analytical methods, pollution characteristics and ecological risks. Trends Anal.

890   Chem. 109, 163-172. doi:10.1016/j.trac.2018.10.006.

891   He, P., Chen, L., Shao, L., Zhang, H., Lü, F., 2019. Municipal solid waste (MSW)

892   landfill: a source of microplastics? -Evidence of microplastics in landfill leachate.

893   Water Res. 159, 38-45. doi:10.1016/j.watres.2019.04.060.

894   Hidayaturrahman, H., Lee, T.-G., 2019. A study on characteristics of microplastic in

895   wastewater of South Korea: identification, quantification, and fate of microplastics

896   during   treatment   process.   Mar.   Pollut.   Bull.   146,   696-702.

897   doi:10.1016/j.marpolbul.2019.06.071.

898   Ho, W.-K., Law, J.C.-F., Zhang, T., Leung, K.S.-Y., 2020. Effects of weathering on the

899   sorption behavior and toxicity of polystyrene microplastics in multi-solute systems.

900   Water Res. 187, 116419. doi:10.1016/j.watres.2020.116419.

901   Horton, A.A., Walton, A., Spurgeon, D.J., Lahive, E., Svendsen, C., 2017.

902   Microplastics in freshwater and terrestrial environments: evaluating the current

903   understanding to identify the knowledge gaps and future research priorities. Sci.

904   Total. Environ. 586, 127-141. doi:10.1016/j.scitotenv.2017.01.190.

905   Hou, L., Kumar, D., Yoo, C.G., Gitsov, I., Majumder, E.L.W., 2021. Conversion and

906   removal strategies for microplastics in wastewater treatment plants and landfills.

907   Chem. Eng. J. 406, 126715. doi:10.1016/j.cej.2020.126715.

908   Huerta Lwanga, E., Thapa, B., Yang, X., Gertsen, H., Salánki, T., Geissen, V., Garbeva,

909   P., 2018. Decay of low-density polyethylene by bacteria extracted from

910   earthworm's guts: a potential for soil restoration. Sci. Total. Environ. 624, 753-

911   757. doi:10.1016/j.scitotenv.2017.12.144.

912   Hujuri, U., Ghoshal, A.K., Gumma, S., 2008. Modeling pyrolysis kinetics of plastic

913   mixtures. Polym. Degrad. Stabil. 93 (10), 1832-1837.

914   doi:10.1016/j.polymdegradstab.2008.07.006.

915   Iñiguez, M.E., Conesa, J.A., Fullana, A., 2018. Recyclability of four types of plastics

916   exposed to UV irradiation in a marine environment. Waste Manage. 79, 339-345.

917   doi:10.1016/j.wasman.2018.08.006.

918   Irina, E., Margarita, B., Andrei, B., Andrei, B., Alexander, K., Irina, P.C., 2018.

919   Secondary microplastics generation in the sea swash zone with coarse bottom

920   sediments: laboratory experiments. Front. Mar. Sci. 5.

921   doi:10.3389/fmars.2018.00313.

922   Jacquin, J., Cheng, J., Odobel, C., Pandin, C., Conan, P., Pujo-Pay, M., Barbe, V.,

923   Meistertzheim, A.L., Ghiglione, J.F., 2019. Microbial ecotoxicology of marine

924   plastic debris: a review on colonization and biodegradation by the "plastisphere".

925   Front. Microbiol. 10, 865. doi:10.3389/fmicb.2019.00865.

926   Julienne, F., Delorme, N., Lagarde, F., 2019a. From macroplastics to microplastics:

927   Role of water in the fragmentation of polyethylene. Chemosphere 236, 124409.

928   doi:10.1016/j.chemosphere.2019.124409.

929   Julienne, F., Lagarde, F., Delorme, N., 2019b. Influence of the crystalline structure on

930   the fragmentation of weathered polyolefines. Polym. Degrad. Stabil. 170, 109012.

41

931   doi:10.1016/j.polymdegradstab.2019.109012.

932   Kholodovych, V., Welsh, W.J., 2007. Thermal-Oxidative Stability and Degradation of

933   Polymers. In: Mark, J.E. (Eds), Physical Properties of Polymers Handbook.

934   Springer, New York, USA, pp. 927-938. doi:10.1007/978-0-387-69002-5_54.

935   Kumar, M., Xiong, X., He, M., Tsang, D.C.W., Gupta, J., Khan, E., Harrad, S., Hou,

936   D., Ok, Y.S., Bolan, N.S., 2020. Microplastics as pollutants in agricultural soils.

937   Environ. Pollut. 265, 114980. doi:10.1016/j.envpol.2020.114980.

938   Lee, Y.K., Murphy, K.R., Hur, J., 2020. Fluorescence signatures of dissolved organic

939   matter leached from microplastics: polymers and additives. Environ. Sci. Technol.

940   54 (19), 11905-11914. doi:10.1021/acs.est.0c00942.

941   Leonas, K.K., 1993. The disintegration rate of traditional and chemically modified

942   plastic films in simulated fresh- and sea-water environments. J. Appl. Polym. Sci.

943   47 (12), 2103-2110. doi:10.1002/app.1993.070471203.

944   Li, C., Busquets, R., Campos, L.C., 2020. Assessment of microplastics in freshwater

945   systems: a review. Sci. Total. Environ. 707, 135578.

946   doi:10.1016/j.scitotenv.2019.135578.

947   Li, Y., Niu, J., Shang, E., Crittenden, J.C., 2015. Synergistic photogeneration of

948   reactive oxygen species by dissolved organic matter and C_{60} in aqueous phase.

949   Environ. Sci. Technol. 49 (2), 965-973. doi:10.1021/es505089e.

950   Liao, C.H., Kang, S.F., Wu, F.A., 2001. Hydroxyl radical scavenging role of chloride

951   and bicarbonate ions in the H_2O_2/UV process. Chemosphere 44 (5), 1193-1200.

952   doi:10.1016/S0045-6535(00)00278-2.

953   Liu, G., Zhu, Z., Yang, Y., Sun, Y., Yu, F., Ma, J., 2019a. Sorption behavior and

954   mechanism of hydrophilic organic chemicals to virgin and aged microplastics in

955   freshwater and seawater. Environ. Pollut. 246, 26-33.

956   doi:10.1016/j.envpol.2018.11.100.

957   Liu, H., Liu, K., Fu, H., Ji, R., Qu, X., 2020a. Sunlight mediated cadmium release from

958   colored microplastics containing cadmium pigment in aqueous phase. Environ.

959   Pollut. 263, 114484. doi:10.1016/j.envpol.2020.114484.

960   Liu, J., Zhang, T., Tian, L., Liu, X., Qi, Z., Ma, Y., Ji, R., Chen, W., 2019b. Aging

961   significantly affects mobility and contaminant-mobilizing ability of nanoplastics

962   in saturated loamy sand. Environ. Sci. Technol. 53 (10), 5805-5815.

963   doi:10.1021/acs.est.9b00787.

964   Liu, M., Lu, S., Song, Y., Lei, L., Hu, J., Lv, W., Zhou, W., Cao, C., Shi, H., Yang, X.,

965   He, D., 2018. Microplastic and mesoplastic pollution in farmland soils in suburbs

966   of Shanghai, China. Environ. Pollut. 242, 855-862.

967   doi:10.1016/j.envpol.2018.07.051.

968   Liu, P., Lu, K., Li, J., Wu, X., Qian, L., Wang, M., Gao, S., 2020b. Effect of aging on

969   adsorption behavior of polystyrene microplastics for pharmaceuticals: Adsorption

970   mechanism and role of aging intermediates. J. Hazard. Mater. 384, 121193.

971   doi:10.1016/j.jhazmat.2019.121193.

972   Liu, P., Qian, L., Wang, H., Zhan, X., Lu, K., Gu, C., Gao, S., 2019c. New insights into

973   the aging behavior of microplastics accelerated by advanced oxidation processes.

974   Environ. Sci. Technol. 53 (7), 3579-3588. doi:10.1021/acs.est.9b00493.

975   Liu, P., Zhan, X., Wu, X., Li, J., Wang, H., Gao, S., 2020c. Effect of weathering on

976   environmental behavior of microplastics: Properties, sorption and potential risks.

977   Chemosphere 242, 125193. doi:10.1016/j.chemosphere.2019.125193.

978   Liu, Y., Hu, Y., Yang, C., Chen, C., Huang, W., Dang, Z., 2019d. Aggregation kinetics

979   of UV irradiated nanoplastics in aquatic environments. Water Res. 163, 114870.

980   doi:10.1016/j.watres.2019.114870.

981 Lucas, N., Bienaime, C., Belloy, C., Queneudec, M., Silvestre, F., Nava-Saucedo, J.E.,

982   2008. Polymer biodegradation: mechanisms and estimation techniques-A review.

983   Chemosphere 73 (4), 429-442. doi:10.1016/j.chemosphere.2008.06.064.

984 Luo, H., Li, Y., Zhao, Y., Xiang, Y., He, D., Pan, X., 2020a. Effects of accelerated

985   aging on characteristics, leaching, and toxicity of commercial lead chromate

986   pigmented   microplastics.   Environ.   Pollut.   257,   113475.

987   doi:10.1016/j.envpol.2019.113475.

988 Luo, H., Xiang, Y., Li, Y., Zhao, Y., Pan, X., 2020b. Weathering alters surface

989   characteristic of TiO_2-pigmented microplastics and particle size distribution of

990   TiO_2 released   into   water.   Sci.   Total.   Environ.   729,   139083.

991   doi:10.1016/j.scitotenv.2020.139083.

992 Luo, H., Xiang, Y., Zhao, Y., Li, Y., Pan, X., 2020c. Nanoscale infrared, thermal and

993   mechanical properties of aged microplastics revealed by an atomic force

994   microscopy coupled with infrared spectroscopy (AFM-IR) technique. Sci. Total.

995   Environ. 744, 140944. doi:10.1016/j.scitotenv.2020.140944.

996 Luo, H., Zhao, Y., Li, Y., Xiang, Y., He, D., Pan, X., 2020d. Aging of microplastics

997   affects their surface properties, thermal decomposition, additives leaching and

998   interactions   in   simulated   fluids.   Sci.   Total.   Environ.   714,   136862.

999   doi:10.1016/j.scitotenv.2020.136862.

1000 Mao, R., Lang, M., Yu, X., Wu, R., Yang, X., Guo, X., 2020. Aging mechanism of

1001   microplastics with UV irradiation and its effects on the adsorption of heavy metals.

1002   J. Hazard. Mater. 393, 122515. doi:10.1016/j.jhazmat.2020.122515.

1003   Mason, S.A., Garneau, D., Sutton, R., Chu, Y., Ehmann, K., Barnes, J., Fink, P.,

1004   Papazissimos, D., Rogers, D.L., 2016. Microplastic pollution is widely detected in

1005   US municipal wastewater treatment plant effluent. Environ. Pollut. 218, 1045-

1006   1054. doi:10.1016/j.envpol.2016.08.056.

1007   Mateos-Cárdenas, A., O'Halloran, J., van Pelt, F.N.A.M., Jansen, M.A.K., 2020. Rapid

1008   fragmentation of microplastics by the freshwater amphipod Gammarus duebeni

1009   (Lillj.). Sci. Rep. 10 (1), 12799. doi:10.1038/s41598-020-69635-2.

1010   McGivney, E., Cederholm, L., Barth, A., Hakkarainen, M., Hamacher-Barth, E.,

1011   Ogonowski, M., Gorokhova, E., 2020. Rapid physicochemical changes in

1012   microplastic induced by biofilm formation. Front. Bioeng. Biotech. 8 (205), 1-14.

1013   doi:10.3389/fbioe.2020.00205.

1014   Mei, W., Chen, G., Bao, J., Song, M., Li, Y., Luo, C., 2020. Interactions between

1015   microplastics and organic compounds in aquatic environments: a mini review. Sci.

1016   Total. Environ. 736, 139472. doi:10.1016/j.scitotenv.2020.139472.

1017   Michels, J., Stippkugel, A., Lenz, M., Wirtz, K., Engel, A., 2018. Rapid aggregation of

1018   biofilm-covered microplastics with marine biogenic particles. Proc. Biol. Sci. 285

1019   (1885). doi:10.1098/rspb.2018.1203.

1020   Mildrexler, D.J., Zhao, M., Running, S.W., 2011. Satellite finds highest land skin

1021   temperatures on Earth. Bull. Am. Meteorol. Soc. 92 (7), 855-860.

1022   doi:10.1175/2011bams3067.1.

1023   Murphy, F., Ewins, C., Carbonnier, F., Quinn, B., 2016. Wastewater treatment works

1024   (WwTW) as a source of microplastics in the aquatic environment. Environ. Sci.

1025   Technol. 50 (11), 5800-5808. doi:10.1021/acs.est.5b05416.

1026   Naik, R.A., Rowles, L.S., Hossain, A.I., Yen, M., Aldossary, R.M., Apul, O.G., Conkle,

1027   J., Saleh, N.B., 2020. Microplastic particle versus fiber generation during photo-

1028   transformation in simulated seawater. Sci. Total. Environ. 736, 139690.

1029   doi:10.1016/j.scitotenv.2020.139690.

1030   Napper, I.E., Bakir, A., Rowland, S.J., Thompson, R.C., 2015. Characterisation,

1031   quantity and sorptive properties of microplastics extracted from cosmetics. Mar.

1032   Pollut. Bull. 99 (1-2), 178-185. doi:10.1016/j.marpolbul.2015.07.029.

1033   Nizzetto, L., Bussi, G., Futter, M.N., Butterfield, D., Whitehead, P.G., 2016. A

1034   theoretical assessment of microplastic transport in river catchments and their

1035   retention by soils and river sediments. Environ. Sci. Process. Impacts 18 (8), 1050-

1036   1059. doi:10.1039/c6em00206d.

1037   Paik, P., Kar, K.K., 2009. Thermal degradation kinetics and estimation of lifetime of

1038   polyethylene particles: Effects of particle size. Mater. Chem. Phys. 113 (2), 953-

1039   961. doi:10.1016/j.matchemphys.2008.08.075.

1040   Paluselli, A., Fauvelle, V., Galgani, F., Sempéré, R., 2019. Phthalate release from

1041   plastic fragments and degradation in seawater. Environ. Sci. Technol. 53 (1), 166-

1042   175. doi:10.1021/acs.est.8b05083.

1043   Panno, S.V., Kelly, W.R., Scott, J., Zheng, W., McNeish, R.E., Holm, N., Hoellein,

1044   T.J., Baranski, E.L., 2019. Microplastic contamination in karst groundwater

1045   systems. Ground Water 57 (2), 189-196. doi:10.1111/gwat.12862.

1046   Pedrotti, M.L., Petit, S., Eyheraguibel, B., Kerros, M.E., Elineau, A., Ghiglione, J.F.,

1047   Loret, J.F., Rostan, A., Gorsky, G., 2021. Pollution by anthropogenic microfibers

1048   in North-West Mediterranean Sea and efficiency of microfiber removal by a

1049   wastewater treatment plant. Sci. Total. Environ. 758, 144195.

1050   doi:10.1016/j.scitotenv.2020.144195.

1051 Pielichowski, K., Njuguna, J. (Eds), 2005. Thermal degradation of polymeric materials,

1052   iSmithers Rapra, Shawbury, UK. pp. 22-29.

1053 Prata, J.C., 2018. Microplastics in wastewater: state of the knowledge on sources, fate

1054   and solutions. Mar. Pollut. Bull. 129 (1), 262-265.

1055   doi:10.1016/j.marpolbul.2018.02.046.

1056 Priyanka, N., Archana, T., 2011. Biodegradability of polythene and plastic by the help

1057   of microorganism: a way for brighter future. Environ. Anal. Toxicol. 1 (4), 2161–

1058   0525. doi:10.4172/2161-0525.1000111.

1059 Ranjan, V.P., Goel, S., 2019. Degradation of low-density polyethylene film exposed to

1060   UV radiation in four environments. J. Hazard. Toxic Radioact. Waste 23 (4),

1061   04019015. doi:doi:10.1061/(ASCE)HZ.2153-5515.0000453.

1062 Resmeriță, A.-M., Coroaba, A., Darie, R., Doroftei, F., Spiridon, I., Simionescu, B.C.,

1063   Navard, P., 2018. Erosion as a possible mechanism for the decrease of size of

1064   plastic pieces floating in oceans. Mar. Pollut. Bull. 127, 387-395.

1065   doi:10.1016/j.marpolbul.2017.12.025.

1066 Rillig, M.C., Ingraffia, R., de Souza Machado, A.A., 2017. Microplastic incorporation

1067   into soil in agroecosystems. Front. Plant. Sci. 8, 1805.

1068   doi:10.3389/fpls.2017.01805.

1069 Robertson, A.R., 1977. The CIE 1976 color-difference formulae. Color Res. Appl 2 (1),

1070   7-11. doi:10.1002/j.1520-6378.1977.tb00104.x.

1071 Romera-Castillo, C., Pinto, M., Langer, T.M., Álvarez-Salgado, X.A., Herndl, G.J.,

1072   2018. Dissolved organic carbon leaching from plastics stimulates microbial

1073   activity in the ocean. Nat. Commun. 9 (1), 1-7. doi:10.1038/s41467-018-03798-5.

1074 Scheurer, M., Bigalke, M., 2018. Microplastics in Swiss floodplain soils. Environ. Sci.

1075   Technol. 52 (6), 3591-3598. doi:10.1021/acs.est.7b06003.

1076   Shabbir, S., Faheem, M., Ali, N., Kerr, P.G., Wang, L.-F., Kuppusamy, S., Li, Y., 2020.

1077   Periphytic biofilm: an innovative approach for biodegradation of microplastics.

1078   Sci. Total. Environ. 717, 137064. doi:10.1016/j.scitotenv.2020.137064.

1079   Singh, B., Sharma, N., 2008. Mechanistic implications of plastic degradation. Polym.

1080   Degrad. Stabil. 93 (3), 561-584. doi:10.1016/j.polymdegradstab.2007.11.008.

1081   Song, Y., Qiu, R., Hu, J., Li, X., Zhang, X., Chen, Y., Wu, W.-M., He, D., 2020.

1082   Biodegradation and disintegration of expanded polystyrene by land snails

1083   *Achatina fulica*. Sci. Total. Environ. 746, 141289.

1084   doi:10.1016/j.scitotenv.2020.141289.

1085   Song, Y.K., Hong, S.H., Jang, M., Han, G.M., Jung, S.W., Shim, W.J., 2017. Combined

1086   effects of UV exposure duration and mechanical abrasion on microplastic

1087   fragmentation by polymer type. Environ. Sci. Technol. 51 (8), 4368-4376.

1088   doi:10.1021/acs.est.6b06155.

1089   Su, Y., Zhang, Z., Wu, D., Zhan, L., Shi, H., Xie, B., 2019. Occurrence of microplastics

1090   in landfill systems and their fate with landfill age. Water Res. 164, 114968.

1091   doi:10.1016/j.watres.2019.114968.

1092   Sun, J., Zhu, Z.-R., Li, W.-H., Yan, X., Wang, L.-K., Zhang, L., Jin, J., Dai, X., Ni, B.-

1093   J., 2021. Revisiting microplastics in landfill leachate: Unnoticed tiny microplastics

1094   and their fate in treatment works. Water Res. 190, 116784.

1095   doi:10.1016/j.watres.2020.116784.

1096   Tang, C.C., Chen, H.I., Brimblecombe, P., Lee, C.L., 2019. Morphology and chemical

1097   properties of polypropylene pellets degraded in simulated terrestrial and marine

1098   environments. Mar. Pollut. Bull. 149, 110626.

1099   doi:10.1016/j.marpolbul.2019.110626.

1100 ter Halle, A., Ladirat, L., Martignac, M., Mingotaud, A.F., Boyron, O., Perez, E., 2017.

1101   To what extent are microplastics from the open ocean weathered? Environ. Pollut.

1102   227, 167-174. doi:10.1016/j.envpol.2017.04.051.

1103 Tian, L., Chen, Q., Jiang, W., Wang, L., Xie, H., Kalogerakis, N., Ma, Y., Ji, R., 2019.

1104   A carbon-14 radiotracer-based study on the phototransformation of polystyrene

1105   nanoplastics in water versus in air. Environ. Sci. Nano. 6 (9), 2907-2917.

1106   doi:10.1039/C9EN00662A.

1107 Tu, C., Chen, T., Zhou, Q., Liu, Y., Wei, J., Waniek, J.J., Luo, Y., 2020. Biofilm

1108   formation and its influences on the properties of microplastics as affected by

1109   exposure time and depth in the seawater. Sci. Total. Environ. 734, 139237.

1110   doi:10.1016/j.scitotenv.2020.139237.

1111 Turgay, E., Steinum, T.M., Colquhoun, D., Karataş, S., 2019. Environmental biofilm

1112   communities associated with early-stage common dentex (*Dentex dentex*) culture.

1113   J. Appl. Microbiol. 126 (4), 1032-1043. doi:10.1111/jam.14205.

1114 Waldman, W.R., De Paoli, M.A., 2008. Photodegradation of

1115   polypropylene/polystyrene blends: styrene–butadiene–styrene compatibilisation

1116   effect. Polym. Degrad. Stabil. 93 (1), 273-280.

1117   doi:10.1016/j.polymdegradstab.2007.09.003.

1118 Wang, C., Xian, Z., Jin, X., Liang, S., Chen, Z., Pan, B., Wu, B., Ok, Y.S., Gu, C.,

1119   2020a. Photo-aging of polyvinyl chloride microplastic in the presence of natural

1120   organic acids. Water Res. 183, 116082. doi:10.1016/j.watres.2020.116082.

1121 Wang, H., Brown, H.R., 2004. Ultraviolet grafting of methacrylic acid and acrylic acid

1122   on high-density polyethylene in different solvents and the wettability of grafted

1123   high-density polyethylene. I. Grafting. Journal of Polymer Science Part A:

1124   Polymer Chemistry 42 (2), 253-262. doi:10.1002/pola.11022.

1125   Wang, L., Wu, W.-M., Bolan, N.S., Tsang, D.C.W., Li, Y., Qin, M., Hou, D., 2021a.

1126   Environmental fate, toxicity and risk management strategies of nanoplastics in the

1127   environment: current status and future perspectives. J. Hazard. Mater. 401, 123415.

1128   doi:10.1016/j.jhazmat.2020.123415.

1129   Wang, Q., Zhang, Y., Wangjin, X., Wang, Y., Meng, G., Chen, Y., 2020b. The

1130   adsorption behavior of metals in aqueous solution by microplastics effected by UV

1131   radiation. J. Environ. Sci. 87, 272-280. doi:10.1016/j.jes.2019.07.006.

1132   Wang, X., Bolan, N., Tsang, D.C.W., Sarkar, B., Bradney, L., Li, Y., 2021b. A review

1133   of microplastics aggregation in aquatic environment: influence factors, analytical

1134   methods, and environmental implications. J. Hazard. Mater. 402, 123496.

1135   doi:10.1016/j.jhazmat.2020.123496.

1136   Wang, X., Li, Y., Zhao, J., Xia, X., Shi, X., Duan, J., Zhang, W., 2020c. UV-induced

1137   aggregation of polystyrene nanoplastics: effects of radicals, surface functional

1138   groups and electrolyte. Environ. Sci. Nano 7 (12), 3914-3926.

1139   doi:10.1039/d0en00518e.

1140   Wang, Y., Wang, X., Li, Y., Li, J., Wang, F., Xia, S., Zhao, J., 2020d. Biofilm alters

1141   tetracycline and copper adsorption behaviors onto polyethylene microplastics.

1142   Chem. Eng. J. 392, 123808. doi:10.1016/j.cej.2019.123808.

1143   Ward, C.P., Armstrong, C.J., Walsh, A.N., Jackson, J.H., Reddy, C.M., 2019. Sunlight

1144   converts polystyrene to carbon dioxide and dissolved organic carbon. Environ. Sci.

1145   Tech. Let. 6 (11), 669-674. doi:10.1021/acs.estlett.9b00532.

1146   Webb, H., Arnott, J., Crawford, R., Ivanova, E., 2012. Plastic degradation and its

1147   environmental implications with special reference to poly(ethylene terephthalate).

1148   Polymers 5 (1), 1-18. doi:10.3390/polym5010001.

1149   Wu, J., Xu, P., Chen, Q., Ma, D., Ge, W., Jiang, T., Chai, C., 2020a. Effects of polymer

1150   aging on sorption of 2,2′,4,4′-tetrabromodiphenyl ether by polystyrene

1151   microplastics. Chemosphere 253, 126706.

1152   doi:10.1016/j.chemosphere.2020.126706.

1153   Wu, X., Liu, P., Huang, H., Gao, S., 2020b. Adsorption of triclosan onto different aged

1154   polypropylene microplastics: critical effect of cations. Sci. Total. Environ. 717,

1155   137033. doi:10.1016/j.scitotenv.2020.137033.

1156   Xu, C., Zhang, B., Gu, C., Shen, C., Yin, S., Aamir, M., Li, F., 2020a. Are we

1157   underestimating the sources of microplastic pollution in terrestrial environment?

1158   J. Hazard. Mater. 400, 123228. doi:10.1016/j.jhazmat.2020.123228.

1159   Xu, Q., Xing, R., Sun, M., Gao, Y., An, L., 2020b. Microplastics in sediments from an

1160   interconnected river-estuary region. Sci. Total. Environ. 729, 139025.

1161   doi:10.1016/j.scitotenv.2020.139025.

1162   Xu, Z., Sui, Q., Li, A., Sun, M., Zhang, L., Lyu, S., Zhao, W., 2020c. How to detect

1163   small microplastics (20–100 μm) in freshwater, municipal wastewaters and

1164   landfill leachates? A trial from sampling to identification. Sci. Total. Environ. 733,

1165   139218. doi:10.1016/j.scitotenv.2020.139218.

1166   Xue, Z., Sendamangalam, V.R., Gruden, C.L., Seo, Y., 2012. Multiple roles of

1167   extracellular polymeric substances on resistance of biofilm and detached clusters.

1168   Environ. Sci. Technol. 46 (24), 13212-13219. doi:10.1021/es3031165.

1169   Yang, J., Cang, L., Sun, Q., Dong, G., Ata-Ul-Karim, S.T., Zhou, D., 2019. Effects of

1170   soil environmental factors and UV aging on Cu^{2+} adsorption on microplastics.

1171   Environ. Sci. Pollut. R. 26 (22), 23027-23036. doi:10.1007/s11356-019-05643-8.

1172   Yousif, E., Haddad, R., 2013. Photodegradation and photostabilization of polymers,

1173   especially polystyrene: Review. SpringerPlus 2 (1), 398. doi:10.1186/2193-1801-

1174   2-398.

1175   Yuan, J., Ma, J., Sun, Y., Zhou, T., Zhao, Y., Yu, F., 2020. Microbial degradation and

1176   other environmental aspects of microplastics/plastics. Sci. Total. Environ. 715,

1177   136968. doi:10.1016/j.scitotenv.2020.136968.

1178   Zhang, B., Yang, X., Chen, L., Chao, J., Teng, J., Wang, Q., 2020a. Microplastics in

1179   soils: A review of possible sources, analytical methods and ecological impacts. J.

1180   Chem. Technol. Biot. 95 (8), 2052-2068. doi:10.1002/jctb.6334.

1181   Zhang, D., Liu , H.B., Li, H.W., Hui, Q.X., Wang, M.X., Rong, Y.C., Yuan, W.H.,

1182   2016. The status and distribution characteristics of residual mulching film in

1183   Xinjiang, China. J. Integr. Agric. 15 (11), 2639-2646. doi:10.1016/S2095-

1184   3119(15)61240-0.

1185   Zhang, D., Liu, X., Huang, W., Li, J., Wang, C., Zhang, D., Zhang, C., 2020b.

1186   Microplastic pollution in deep-sea sediments and organisms of the Western Pacific

1187   Ocean. Environ. Pollut. 259, 113948. doi:10.1016/j.envpol.2020.113948.

1188   Zhang, G.S., Liu, Y.F., 2018. The distribution of microplastics in soil aggregate

1189   fractions in southwestern China. Sci. Total. Environ. 642, 12-20.

1190   doi:10.1016/j.scitotenv.2018.06.004.

1191   Zhang, J., Gao, D., Li, Q., Zhao, Y., Li, L., Lin, H., Bi, Q., Zhao, Y., 2020c.

1192   Biodegradation of polyethylene microplastic particles by the fungus *Aspergillus*

1193   *flavus* from the guts of wax moth *Galleria mellonella*. Sci. Total. Environ. 704,

1194   135931. doi:10.1016/j.scitotenv.2019.135931.

1195   Zhang, J., Wang, L., Halden, R.U., Kannan, K., 2019. Polyethylene terephthalate and

1196   polycarbonate microplastics in sewage sludge collected from the United States.

1197   Environ. Sci. Tech. Let. 6 (11), 650-655. doi:10.1021/acs.estlett.9b00601.

1198   Zhang, K., Hamidian, A.H., Tubić, A., Zhang, Y., Fang, J.K.H., Wu, C., Lam, P.K.S.,

1199   2021. Understanding plastic degradation and microplastic formation in the

1200   environment: a review. Environ. Pollut. 274, 116554.

1201   doi:10.1016/j.envpol.2021.116554.

1202   Zhang, L., Xie, Y., Liu, J., Zhong, S., Qian, Y., Gao, P., 2020d. An overlooked entry

1203   pathway of microplastics into agricultural soils from application of sludge-based

1204   fertilizers. Environ. Sci. Technol. 54 (7), 4248-4255. doi:10.1021/acs.est.9b07905.

1205   Zhang, S., Liu, X., Hao, X., Wang, J., Zhang, Y., 2020e. Distribution of low-density

1206   microplastics in the mollisol farmlands of northeast China. Sci. Total. Environ.

1207   708, 135091. doi:10.1016/j.scitotenv.2019.135091.

1208   Zhou, Q., Jin, Z., Li, J., Wang, B., Wei, X., Chen, J., 2018. A novel air-assisted liquid-

1209   liquid microextraction based on in-situ phase separation for the HPLC

1210   determination of bisphenols migration from disposable lunch boxes to contacting

1211   water. Talanta 189, 116-121. doi:10.1016/j.talanta.2018.06.072.

1212   Zhu, K., Jia, H., Sun, Y., Dai, Y., Zhang, C., Guo, X., Wang, T., Zhu, L., 2020a. Long-

1213   term phototransformation of microplastics under simulated sunlight irradiation in

1214   aquatic environments: Roles of reactive oxygen species. Water Res. 173, 115564.

1215   doi:10.1016/j.watres.2020.115564.

1216   Zhu, L., Zhao, S., Bittar, T.B., Stubbins, A., Li, D., 2020b. Photochemical dissolution

1217   of buoyant microplastics to dissolved organic carbon: rates and microbial impacts.

1218   J. Hazard. Mater. 383, 121065. doi:10.1016/j.jhazmat.2019.121065.

1219 Ziajahromi, S., Neale, P.A., Rintoul, L., Leusch, F.D.L., 2017. Wastewater treatment

1220   plants as a pathway for microplastics: development of a new approach to sample

1221   wastewater-based   microplastics.   Water   Res.   112,   93-99.

1222   doi:10.1016/j.watres.2017.01.042.

1223 Ziajahromi, S., Neale, P.A., Telles Silveira, I., Chua, A., Leusch, F.D.L., 2021. An audit

1224   of microplastic abundance throughout three Australian wastewater treatment

1225   plants. Chemosphere 263, 128294. doi:10.1016/j.chemosphere.2020.128294.

1226 Zweifel, H. (Eds) 1999. Stabilization of polymeric materials, Springer, Berlin,

1227   Germany. pp. 3-4. doi:10.1016/S0151-9107(99)80080-4.

1228

1229   **Figures**
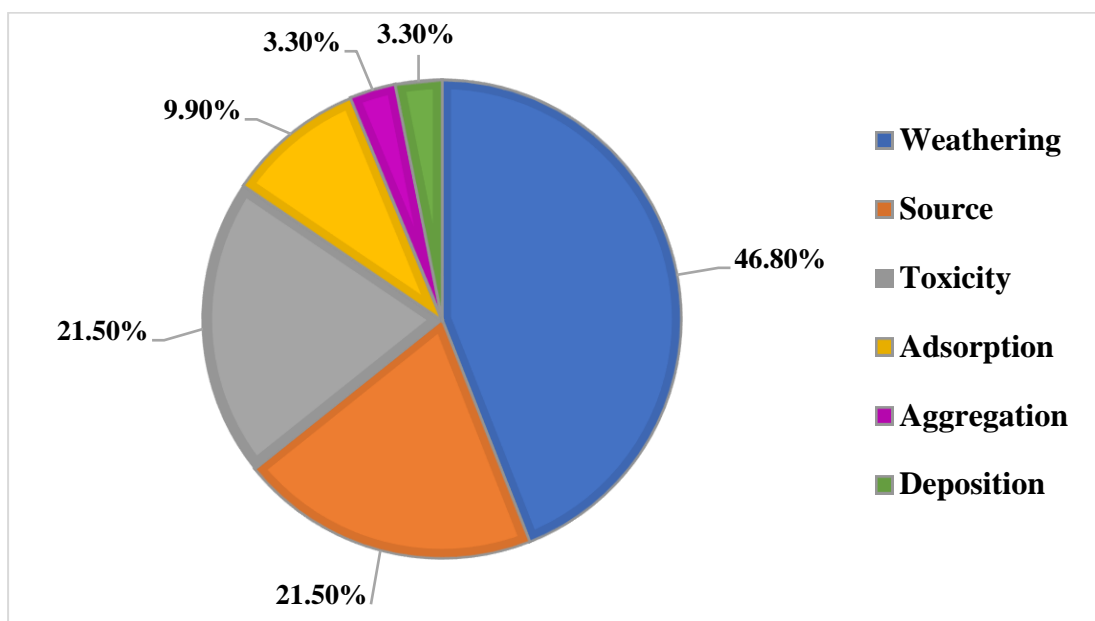
1230

1231
1232   **Fig. 1.** The proportion of research papers up to February 2021 investigating the
1233   transport and transformation of microplastics.
1234

Initiation $RH \xrightarrow[\text{Photo-degradation}]{\text{ROS}} R\bullet \xleftarrow[\text{Thermal/Photo-degradation}]{\text{heat}/hv} RH$

$\downarrow O_2$

Propagation $HO_2\bullet + R\bullet \xleftarrow[RH]{hv} ROO\bullet \xrightarrow[RH]{\text{heat}/hv} ROOH$

$\downarrow HO_2\bullet$

H_2O_2

$RO\bullet$ $R\bullet/ROO\bullet \xleftarrow[\text{RH/ROOH}]{\text{heat}/hv} \bullet OH$

heat/hv heat/hv

$\downarrow RH$	$\downarrow$ β-scission	$\downarrow$ β-scission
ROH	R_1-CO-R_2	R_1-CHO

+   Norrish I /hv hv \ Norrish II

$R\bullet$ $R_1-CO\bullet + R_2\bullet$ $R_1-CO-CH_3$

Termination   Olefins, Aldehydes, Ketones……

hv | Mineralization

$CO_2 + H_2O$
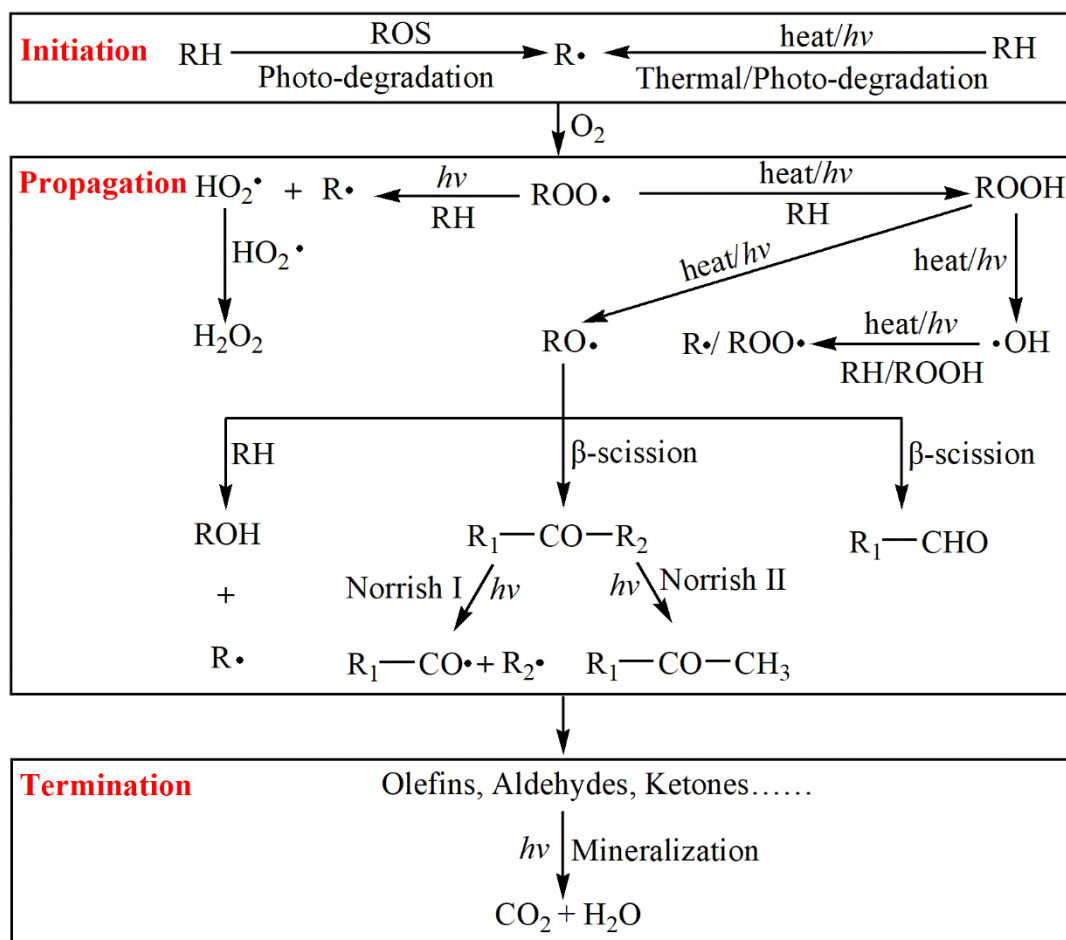
Scheme 1. Thermal-degradation and photo-degradation pathways of microplastics (RH represents microplastics; R_1 and R_2 represent different polymer chains of variable lengths).
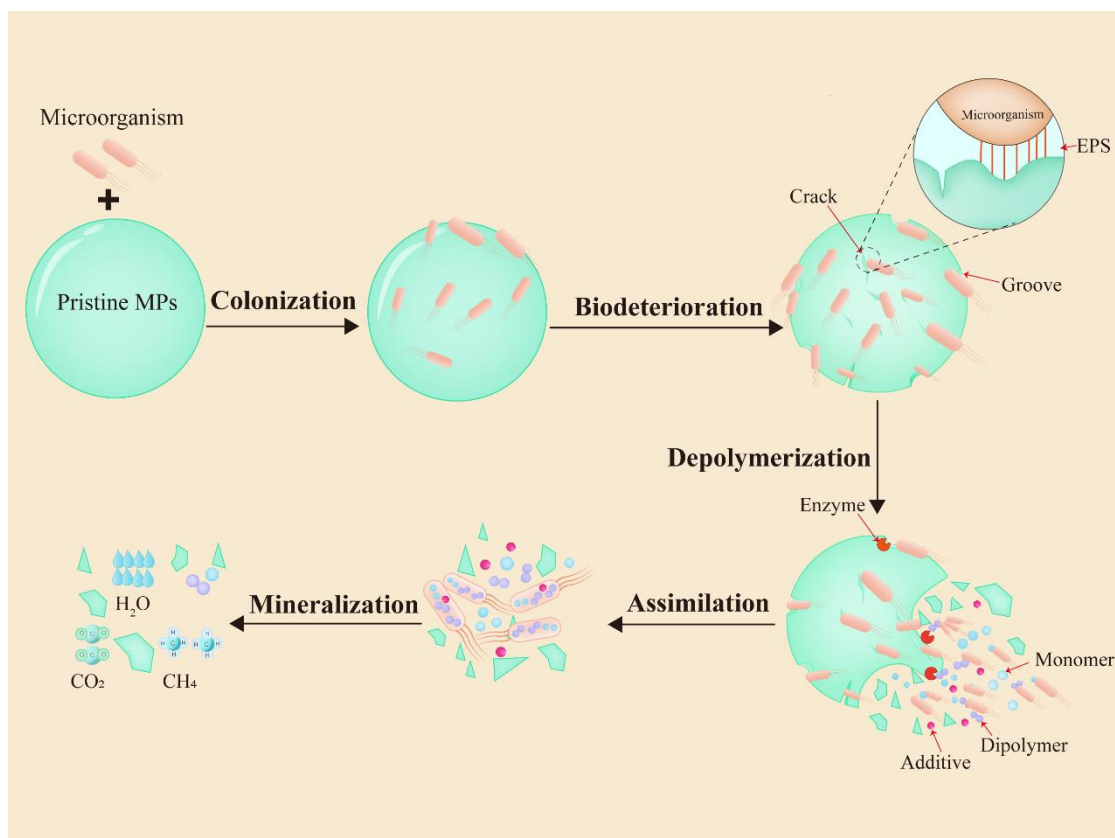
1242

1243

1244 **Fig. 2.** Microbial degradation pathway of microplastics by microorganisms (EPS
1245 presents extracellular polymeric substances).
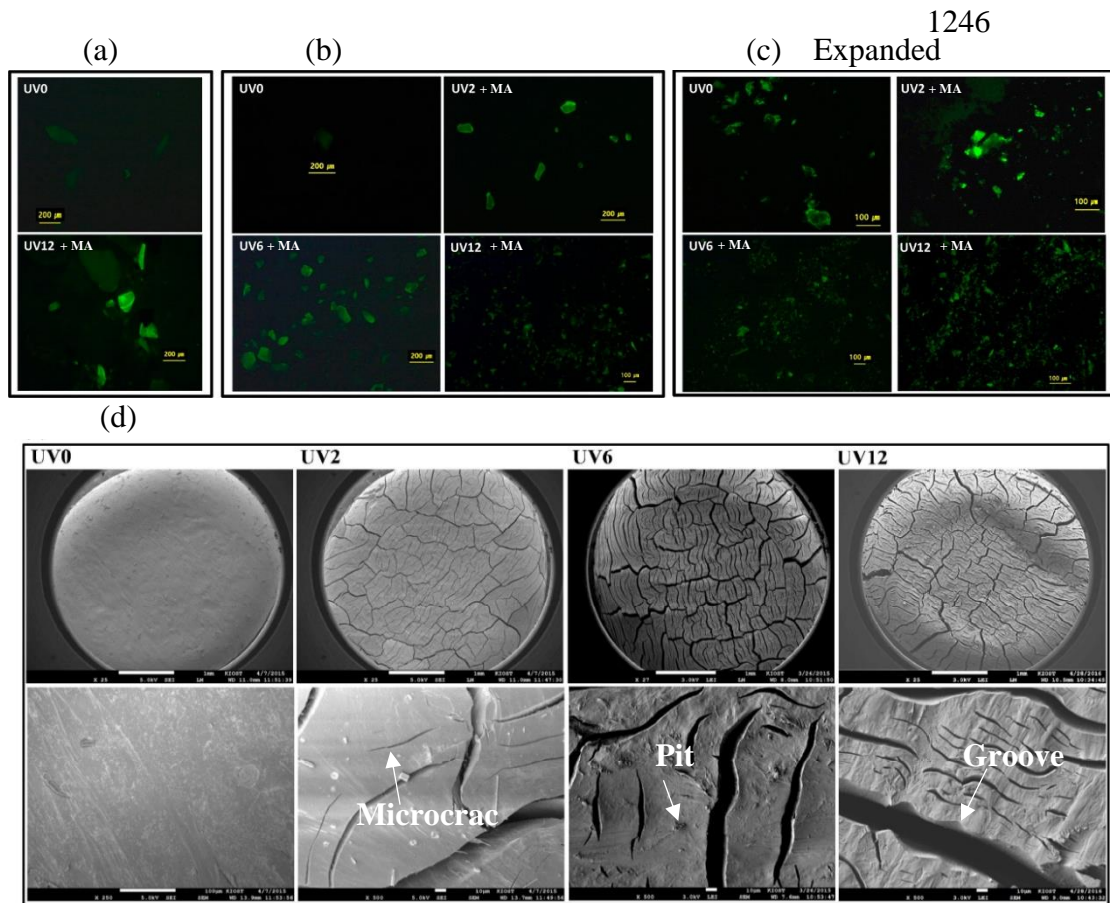
Fig. 3. Fluorescent images of fragment of (a) polyethylene (PE), (b) polypropylene (PP), and (c) expanded polystyrene (PS) MPs after different UV exposure time (0, 2, 6, 12 months) and subsequent mechanical abrasion (MA) by sand (2 months); (d) SEM images of PP after different UV exposure time (0, 2, 6, 12 months). UV0, UV2, UV6 and UV12 represent UV exposure time for 0, 2, 6 and 12 months. Graph was cited and reproduced from "Combined effects of UV exposure duration and mechanical abrasion on microplastic fragmentation by polymer type" (Song et al., 2017) with permission.

1256
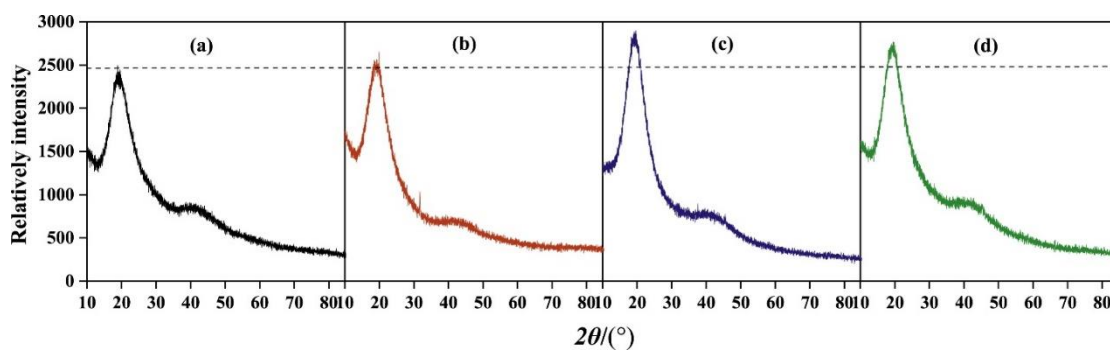
1257

1258   **Fig. 4.** The XRD patterns of (a) pristine PS, (b) aged PS via seawater soaking, (c) aged
1259   PS via UV irradiation and (d) aged PS via concurrent seawater soaking and UV
1260   irradiation. Graph was cited and reproduced from "Effects of polymer aging on sorption
1261   of 2,2′,4,4′-tetrabromodiphenyl ether by polystyrene microplastics" (Wu et al., 2020)
1262   with permission.
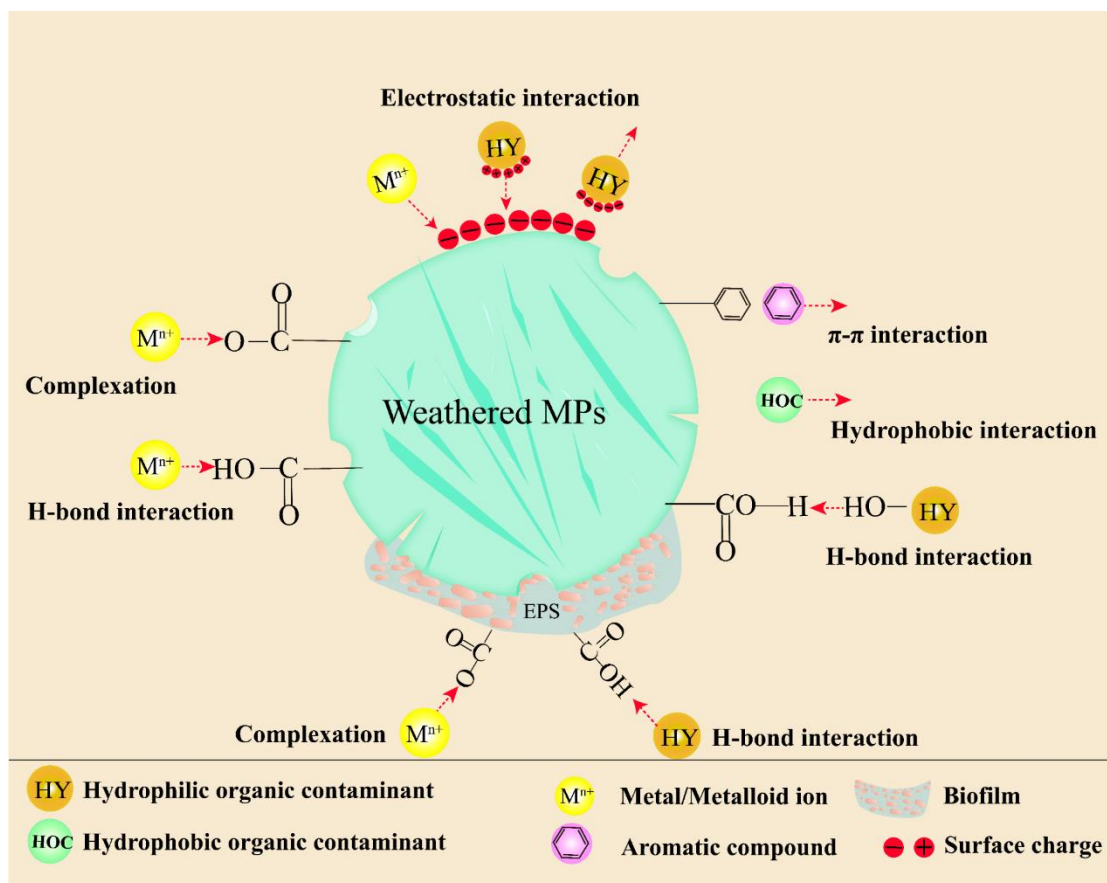
1263

1264

1265 **Fig. 5.** Interaction between weathered microplastics and organic/inorganic
1266 contaminants (the arrows pointing to and away from the weathered microplastics
1267 represent the promotion and inhibition of sorption, respectively).
1268

1269 -
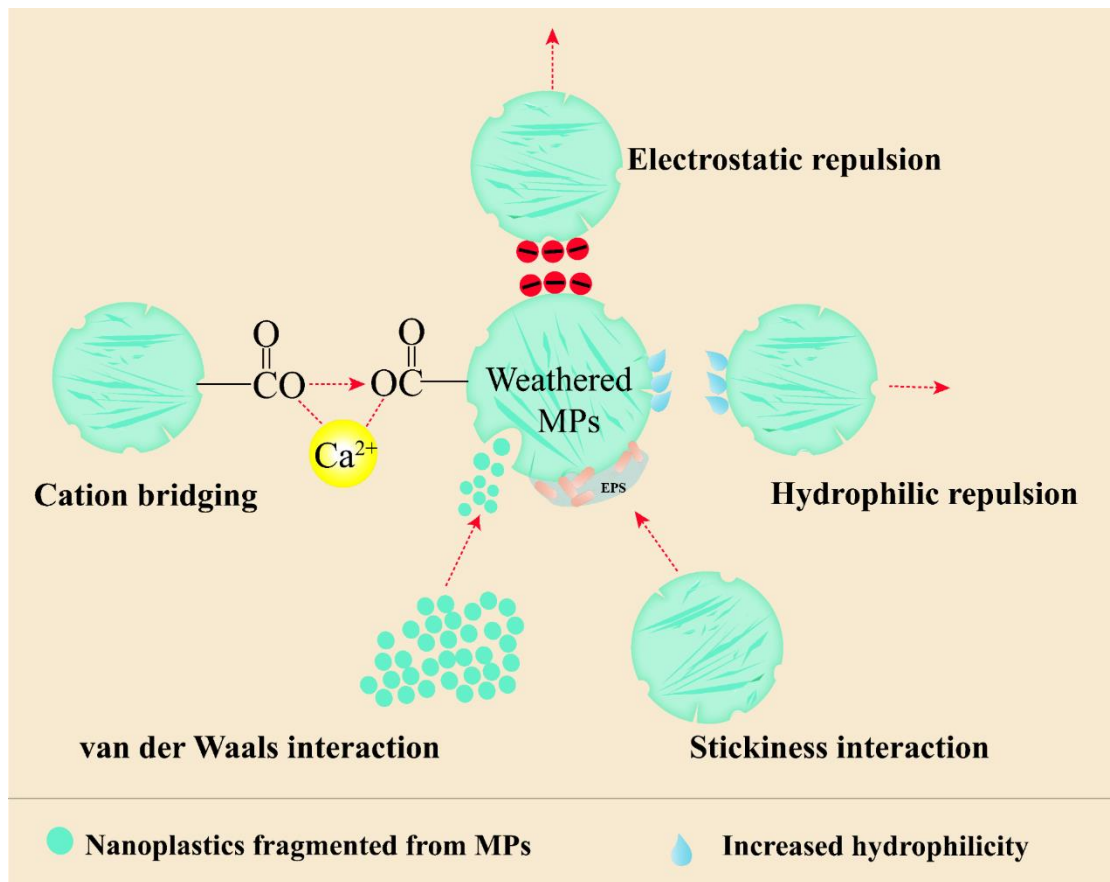
1270

1271

1272 **Fig. 6.** Homo-aggregation of weathered microplastics (The arrows pointing to and away
1273 from the weathered microplastics represent the promotion and inhibition of aggregation,
1274 respectively, EPS represents extracellular polymeric substances).
1275

1276

Tables

Table 1. The types, sizes and concentrations of MPs from different sources in terrestrial and aquatic environments.

Environment	Source	Sample site	Type	Size	Average concentration	Reference
Terrestrial environments	Landfill refuse	Laogang landfill, Shanghai, China	PP, PE, PS, PEUR, EPM	0.23-4.97 mm	62 items g^{-1} (dw)	(Su et al., 2019)
	Landfill leachate	Laogang landfill, Shanghai, China	PP, PE, PS, cellophane	0.07-3.67 mm	8 items L^{-1}	(Su et al., 2019)
		Landfills, Shanghai, Wuxi, Suzhou and Changzhou, China	PP, PE	0.1-1 mm	5.08 items L^{-1}	(He et al., 2019)
		Landfills, Shanghai, China	PP, PA, Rayon	0.02-0.1 mm	291 items L^{-1}	(Xu et al., 2020c)
	Biosolids	Dewatered sludge of WWTPs, Guilin, China	PP, PE	0.2-5 mm	2.2-5.2 items g^{-1} (dw)	(Zhang et al., 2020d)
		Agricultural fields underwent sludge applications, Mellipilla, Chile	N.D.	N.D.	0.6-10.4 items g^{-1} (dw)	(Corradini et al., 2019)
	Plastic mulches [a]	Agricultural lands, Xinjiang, China	N.D.	N.D.	502.2 kg ha^{-1} (maximum)	(Zhang et al., 2016)
		Agricultural lands, Yunnan, China	N.D.	0.05-5 mm	18.8 items g^{-1} (dw)	(Zhang and Liu, 2018)
Aquatic environments	Effluent of WWTPs	Glasgow, UK	PP, PE, PET, PA, PS, PES	0.6-1.6 mm	0.25 items L^{-1}	(Murphy et al., 2016)
		Sydney, Australia	PP, PE, PET, PA, PS	0.025-5 mm	0.21-1.6 items L^{-1}	(Ziajahromi et al., 2017)
		Australia	PP, PE, PET, PA	0.025-5 mm	0.18-1.91 items L^{-1}	(Ziajahromi et al., 2021)
		Daegu, South Korea	N.D.	0.03-1.5 mm	33-297 items L^{-1}	(Hidayaturrahman and Lee, 2019)

Note: Ethylene-propylene copolymer (EPM), Polyether urethane (PEUR), Polyester (PES), Polypropylene (PP), Polystyrene (PS), Polyethylene (PE), Polyethylene terephthalate (PET), Polyamide (PA), Wastewater treatment plants (WWTPs). N.D. represented no data. [a] represented plastic mulches residual rather than MPs.

Table 2. Review of recent studies regarding the weathering processes of MPs in-situ or in laboratory.

Weathering process	MPs	Experimental conditions				Key conclusions	Reference
		Size	Time	Matrix	Method		
Mechanical fragmentation	Polyolefin	398 ± 54 nm	180 s	Water	Broken by mechanical impeller, horn sonicator, hydraulic pump	Water shear forces promote nanoplastic (< 10 nm) generation mainly by crack propagation and crushing mechanism.	(Enfrin et al., 2020)
	PE, PP, expanded PS	26 ± 0.8 mm^3, 19 ± 0.9 mm^3, 20 ± 2.2 mm^3	2 months	Sand	Ground by roller mixer	Expanded PS pellets are more susceptible to fragmentation than PE and PP, due to the lower mechanical strength of Expanded PS.	(Song et al., 2017)
	PE	6 mm $\times 2$ mm	30 d	Simulated seawater	Ground in a wave tank with UV light	Secondary MPs (1-2.4 μm^2) account for an increasing proportion with the increasing of weathering time.	(Resmeriță et al., 2018)
Photo-degradation	LDPE	< 500 μm	42 d	Air, 69% humidity	Xenon lamp (120 mW cm^{-2})	Aged-MPs had a rougher surface, lower glass transition temperature, and higher surface stiffness.	(Luo et al., 2020c)
	PS	150 μm	150 d	Ultrapure water	Simulated sunlight (68.25 mW cm^{-2})	Reactive oxide species played a major role in the photodegradation process of PS MPs in their aqueous suspension.	(Zhu et al., 2020a)
	^{14}C-PS	250 ± 88 nm	2 d	Distilled water/air	UV-254 nm (0.7 mW cm^{-2})	The mineralization efficiency of PS in water were higher ($17.1 \pm 0.55\%$) than in air ($6.17 \pm 0.1\%$).	(Tian et al., 2019)
	PP, PS, PE	N.D.	3 months	Simulated seawater/ultrapure water/air	UV 340 nm	The weathering degree of MPs decreased in the order of air < ultrapure water < seawater, depending on the irradiation time, oxygen content, and water salinity.	(Cai et al., 2018)

Weathering process	MPs	Experimental conditions				Key conclusions	Reference
		Size	Time	Matrix	Method		
	PE	< 500 μm	56 d	Air, 50% humidity	Xenon-lamp (120 mW cm^{-2})	Aged MPs resulted in color change, decrease of high temperature resistance, and increase of CI value.	(Luo et al., 2020d)
	HDPE, PA, PP, HIPS	2 mm	5 d	Simulated seawater	253.7 nm	UV-induced shape (fiber and particle) of secondary MPs depends on plastic types. HDPE and nylon 6 mainly generated MP fibers, while HIPS and PP were more resistant to photo-transformation.	(Naik et al., 2020)
Thermal-degradation	PS	< 500 μm	56 d	Compost suspension	70 °C	High temperature (70 °C) caused the formation of cracks, whereas no obvious change occurred at 40 °C.	(Chen et al., 2020)
	PS	1 μm	3 months	Simulated seawater/ ultrapure water/air	75 °C	The aging mechanisms of PS were different in the three aging conditions according to sequence of aged functional groups.	(Ding et al., 2020)
	PP	5 mm	0.5 h	Purified water	121 °C	The leaching rate of BPA increased with higher temperature.	(Zhou et al., 2018)
Biodegradation	UV-aged PP	2.4 mm	40 d	Liquid medium	Isolated microorganism from sediments of mangrove	The weight losses of PP after biodegradation by *Rhodococcus* and *Bacillus* were 6.4% and 4.0%, respectively.	(Auta et al., 2018)
	PE *	3-5 mm	135 d	Seawater from Yellow Sea	Biofilm	The thickness of biofilms on PE surface increased with prolonging of exposure time (30, 75, and 135 days), but decreased with deeper natural coastal water (2 m, 6 m, and 12 m).	(Tu et al., 2020)

Weathering process	MPs	Experimental conditions				Key conclusions	Reference
		Size	Time	Matrix	Method		
	HDPE	< 200 μm	28 d	Liquid medium	Isolated microorganisms from wax moth guts	*Aspergillus flavus* was isolated, and the fungus degraded PE with the mass loss percentage of 3.90 ± 1.18%.	(Zhang et al., 2020c)
	LDPE	< 150 μm	21 d	Sandy soil	Isolated microorganisms from earthworm gut	Gram-positive bacteria, including phylum Actinobacteria and Firmicutes, were isolated from the earthworm's gut, and they resulted in weight loss of 60%. Furthermore, several long-chain alkanes were detected in the bio-treatment.	(Huerta Lwanga et al., 2018)
	MPs *	N.D.	45 d	Sludge	Composting with high temperature (70-90 ℃)	The degradation efficiency (weight loss percentages) of MPs was 43.7%.	(Chen et al., 2020)
	PS	< 500 μm	56 d	Liquid medium	Isolated microorganisms from sludge	The degradation efficiency (weight loss percentages) of PS MPs was 7.3 % and 1.1% at 70 °C and 40 °C after 56 days, respectively.	(Chen et al., 2020)

Note: Bisphenol A (BPA), Carbonyl index (CI), High impact PS (HIPS), High density polyethylene (HDPE), Low density polyethylene (LDPE), Polypropylene (PP), Polystyrene (PS), Polyethylene (PE), Polyamide (PA), Polyethylene terephthalate (PET). * represented the *in-situ* experiment of MP weathering process. N.D. represented no data.

Table 3. The types and concentrations of released chemicals from weathered MPs.

Type of chemicals	Released chemicals	Concentration	MP type	Source	Weathering process	Reference
Additive	EDC	1.10 and 0.25 µg g^{-1} for small (0.5-1.5 mm) and medium (1.5-5 mm) MPs, respectively	PE	The North Pacific Subtropical Gyre	Natural weathering	(Chen et al., 2019b)
	DiBP, DnBP	0.083, 0.120 µg g^{-1}	PE	Plastic garbage bag	Artificial light weathering	(Paluselli et al., 2019)
	BPS, BPAF	0.012, 0.070 µg g^{-1}	PP	Disposable plastic boxes	Thermal weathering (121 ℃)	(Zhou et al., 2018)
	DMP, DEP	0.010, 0.069 µg g^{-1}	PVC	Insulation layer of electric cables	Artificial light weathering	(Paluselli et al., 2019)
	DMT, DBT	1.51-14.48, 1.03-4.55 µg g^{-1}	PVC	Thin sheet	UV 365 nm weathering	(Chen et al., 2019a)
	THMs	90-454 µg L^{-1}	PE, PP, PLA, PMMA, PS	Commercial products	UV 340 nm weathering	(Ateia et al., 2020)
	Cr (VI) Pb (II)	12.1, 81.4 µg g^{-1}	PE	Raw plastic masterbatches	Xenon lamp weathering (120 mW cm^{-2})	(Luo et al., 2020a)
	Cd (II)	98.95 µg g^{-1}	PP	Plastic buckets	Xenon lamp weathering (61.5-70.6 mW cm^{-2})	(Liu et al., 2020a)
Monomer	TPA	0.085-75 µg g^{-1} (dw)	PET	Sewage sludge	Natural weathering	(Zhang et al., 2019)
	BPA	0.0083-2.5 µg g^{-1} (dw)	PC	Sewage sludge	Natural weathering	(Zhang et al., 2019)
Oxygenated	TOC	7130 µg L^{-1}	PS	Synthetic MPs	UV 254 nm weathering	(Tian et al., 2019)

Type of chemicals	Released chemicals	Concentration	MP type	Source	Weathering process	Reference
compounds					(0.7 mW cm^{-2})	
	DOC	$2870 \ \mu g \ L^{-1}$	PS	Sigma-Aldrich corporation	UVA weathering (4 mW cm^{-2})	(Lee et al., 2020)
	DOC	$6.0, 1.12 \ \mu g \ cm^{-2}$	LDPE, HDPE	GoodFellow	Artificial light weathering	(Romera-Castillo et al., 2018)
	DOC	$1280 \ \mu g \ L^{-1}$	PVC	Sigma-Aldrich corporation	UVA weathering (4 mW cm^{-2})	(Lee et al., 2020)

Note: Bisphenol A (BPA), Bisphenol AF (BPAF), Bisphenols (BPS), Dimethyltin byproducts (DMT), Disinfection byproducts (DBP), Dimethyl phthalate (DMP), Diethyl phthalate (DEP), Di-isobutyl phthalate (DiBP), Di-n-butyl phthalate (DnBP), Dibutyltin (DBT), Dissolved organic carbon (DOC), Endocrine disrupting chemicals (EDC), High density polyethylene (HDPE), Low density polyethylene (LDPE), Polyethylene (PE), Polypropylene (PP), Polystyrene (PS), Polyvinylchloride (PVC), Poly (methyl methacrylate) (PMMA), Polylactic acid (PLA), Polyethylene terephthalate (PET), Polycarbonate (PC), Terephthalic acid (TPA), Trihalomethanes (THMs), Total organic carbon (TOC).